MINISTRY OF INDUSTRY & TRADE
INDUSTRIAL R & D ADMINISTRATION
משרד התעשיה והמסחר
המינהל למחקר ופיתוח תעשייתי

ISRAEL INSTITUTE OF METALS · מכון המתכות הישראלי

TECHNION RESEARCH AND DEVELOPMENT FOUNDATION LTD.
מעד הטכניון למחקר ופיתוח בע"מ

Laser and Electrochemical Studies of Metallization in Electronic Devices

J. Zahavi, M. Rotel
Israel Institute of Metals

B. Dobbs, AFWAL/MLSA
Wright-Patterson AFB

Interim Scientific Report

September 1, 1987 — August 31, 1988

Prepared for

EOARD — London, England

AFOSR, BOLLING AFB, Washington. D. C. 20332, U. S. A.

LASER AND ELECTROCHEMICAL STUDIES OF METALLIZATION IN ELECTRONIC DEVICES

J. Zahavi, M. Rotel

Israel Institute of Metals
Technion, Haifa, Israel

and

B. Dobbs, AFWAL/MLSA

Wright-Patterson AFB
Ohio, 45433, U.S.A.

AFOSR GRANT 86-0315
TECHNION NO. 5045 -91

Intrim Scientific Report
September 1, 1987 - August 31, 1988

Prepared for

EOARD - London, England
AFOSR, BOLLING AFB, Washington D.C. 20332, U.S.A.

UNCLASSIFIED

SECURITY CLASSIFICATION OF THIS PAGE

REPORT DOCUMENTATION PAGE

Form Approved OMB No. 0704-0188

1a. REPORT SECURITY CLASSIFICATION: UNCLASSIFIED	1b. RESTRICTIVE MARKINGS
2a. SECURITY CLASSIFICATION AUTHORITY	3. DISTRIBUTION/AVAILABILITY OF REPORT: Approved for public release; Distribution unlimited
2b. DECLASSIFICATION/DOWNGRADING SCHEDULE	
4. PERFORMING ORGANIZATION REPORT NUMBER(S): 2-504591	5. MONITORING ORGANIZATION REPORT NUMBER(S)
6a. NAME OF PERFORMING ORGANIZATION: Israel Institute of Metals, Technion. / 6b. OFFICE SYMBOL (If applicable)	7a. NAME OF MONITORING ORGANIZATION: European Office of Aerospace Research and Development
6c. ADDRESS (City, State, and ZIP Code): Technion City, Haifa, 32 000 Israel.	7b. ADDRESS (City, State, and ZIP Code): Box 14 FPO New York 09510-0200
8a. NAME OF FUNDING/SPONSORING ORGANIZATION: EOARD and AFWAL / 8b. OFFICE SYMBOL (If applicable): LRC & MLSE	9. PROCUREMENT INSTRUMENT IDENTIFICATION NUMBER: AFOSR-86-0315
8c. ADDRESS (City, State, and ZIP Code): Box 14, FPO New York 09510-0200 and Wright-Patterson AFB, OH 45433-6523	10. SOURCE OF FUNDING NUMBERS: PROGRAM ELEMENT NO. / PROJECT NO. / TASK NO. / WORK UNIT ACCESSION NO.

11. TITLE (Include Security Classification): Laser and Electrochemical Studies of Metallizations in Electronic Devices.

12. PERSONAL AUTHOR(S): J. Zahavi, M. Rotel, B. Dobbs.

13a. TYPE OF REPORT	13b. TIME COVERED	14. DATE OF REPORT (Year, Month, Day)	15. PAGE COUNT
Itrim Scientific	FROM Sept.87 TO Aug.88	15th Nov. 88	81

16. SUPPLEMENTARY NOTATION

17. COSATI CODES			18. SUBJECT TERMS (Continue on reverse if necessary and identify by block number)
FIELD	GROUP	SUB-GROUP	Yttrium-Barium-Copper-Oxide

19. ABSTRACT (Continue on reverse if necessary and identify by block number)

In the current study a major effort was conducted in finding suitable methods of metallization of superconductor Y-Ba-Cu-O base ceramic material to form low ohmic contact resistance without annealing and masking procedure. The authors introduced the procedure of laser induced metallization from plating solution on immersed substrate without the need of external power and masking procedure. The feasibility of laser induced high speed, high selective metal (gold) deposit from nonaqueous gold plating solution on superconductive ceramic material was shown. Patterned metallization of gold deposit show low resistance ohmic contact which decreases with decrease of temperature. (AHK

20. DISTRIBUTION/AVAILABILITY OF ABSTRACT	21. ABSTRACT SECURITY CLASSIFICATION
■ UNCLASSIFIED/UNLIMITED ☐ SAME AS RPT. ☐ DTIC USERS	UNCLASSIFIED
22a. NAME OF RESPONSIBLE INDIVIDUAL: Dr. Bill Dobbs	22b. TELEPHONE (Include Area Code): (513) 255-3487 / 22c. OFFICE SYMBOL: AFWAL/MLSE

DD Form 1473, JUN 86 — Previous editions are obsolete. — SECURITY CLASSIFICATION OF THIS PAGE

UNCLASSIFIED

TABLE OF CONTENTS

TABLE OF CONTENTS (Continued)

LIST OF TABLES AND FIGURES

LIST OF TABLES AND FIGURES (Continued)

LIST OF TABLES AND FIGURES (Continued)

1.0 INTRODUCTION

1.1 General

Since January 1986 with the finding of Bendorz and Muller [1] of superconducting oxide ceramic materials of barium lanthanum and copper at 30°K series of investigations have been followed and super conductivity at 90°K or more was reported for ceramic bulk materials of Y-Ba-Cu-O systems [2-7]. At this range of temperature (90°K) liquid helium could be replaced by liquid nitrogen which is cheaper and long lasting.

Various conditions were employed in preparing bulk ceramic superconductor materials. These included mixing of Y_2O_3, CuO and $BaCo_3$, prefiring, grinding processing, firing and slowly cooling in an oxygen at atmosphere [4,5]. By now the preparation of bulk Y-Ba-Cu-O base superconducting ceramic samples has been well established and reproduced by many groups [1,7].

The discovery of superconductivity around 90°K in the Y-Ba-Cu-O ceramic system has developed a great deal of interest in the practical applications of the stable compound $Y\text{-}Ba_2\text{-}Cu_3\text{-}O_7$ known as 1:2:3 compound. Applications of high temperature superconductor (HTSC) materials could be found in microelectronic devices, sensors, power transmission lines, electronic interconnects and many others.

However a major obstacle in the processes of applications of HTSC materials is the contact resistance which is formed where external metallic leads are attached to the HTSC surface.

Recently several researchers [8,9,10] addressed the contact resistance problem.

Contact surface resistivity in the order of 10^{-2} to $10\ \Omega \times Cm^2$ was obtained with contacts made with Indium, silver paint, direct wire bonds and pressure bonds [8,9]. In recent studies [8-10] it was found that silver and gold contacts on superconductive Y-Ba-Cu-O base material showed low ohmic contact resistance in the range of $10^{-10}\Omega \times Cm^2$. That low range of contact resistance was achieved only after annealing the contacts at one atmosphere of oxygen during one hour at 500°C and 600°C for silver and gold respectively. It might be noted that the gold was deposited by sputtering technique [9,10] while the silver by thermal evaporator [8]. No major efforts have been invested to find such methods and mode of formation of low resistance ohmic contacts without the need for annealing as well as avoiding high vacuum, high temperature, high voltage and masking operation while depositing and forming the metallic contact.

In the current study therefore a major effort was conducted in finding suitable methods of metalization of superconductor Y-Ba-Cu-O base ceramic material to form low ohmic contact resistance without annealing and masking procedure.

The authors introduced the procedure of laser induced metallization from plating solution on immersed substrate without the need of external power and masking procedure.

Metallization via pulse laser irradiation have been already shown on semiconductor substrates [11-15] and polymers [11]. Following previous experience with semiconductors and polymers the metallization via pulse laser irradiation on superconductor ceramic base material was explored and investigated in the current study.

1.2 Objectives

The main objectives of this study were:

A. To establish a high speed, direct, selective metallization process at ambient temperature on superconductive ceramic materials for low resistance ohmic contacts and conductive lines.

B. Making use of pulsed laser irradiation for metal or alloy deposition on superconductive ceramic material immersed in non-water based plating solution without external power and without masking procedures.

c. Characterizing formation condition such as mode of pulse laser operation, laser energy intensity, wavelength, number of pulses and type of plating solution to give desired metallization patterns with desired electrical properties.

1.3 Significance

A. Replacing conventional metallization processes such as sputtering, thermal evaporator by high speed, direct, one step, selective laser writing on high Tc superconductive ceramic materials immersed in non-water base plating solution.

B. Direct formation of low ohmic electrical resistance contacts on HTSC without pre and post surface treatment or annealing procedure.

2.0 EXPERIMENTAL

2.1 Experimental Set-Up

The experimental set-up used in this work consisted of three basic systems: (A) a pulsed laser systems, (B) an electroplating solution cell mounted on a computerized X-Y table, and (C) a computer controlling the movement of the X-Y table as well as synchronizing the laser irradiation with the table movement.

A schematic drawing of the overall system is shown in Figure 2.1 A Q-switch pulse YAG laser system was used in this study. However it might be noted that pulsed uv laser system would be also suitable for that work as shown previously by one of the authors (J.Z.) in unpublished work.

2.1.1 Laser System

The laser system used in this study was a Q-switch YAG laser made by Qunatel Company, operating under the following conditions:

Irradiation Wavelength: 532 nm, 1060 nm

Laser Energy per Pulse: up to 5 mj/pulse

Pulse Duration: 15 ns

Repetition Rate: Up to 10 Hz

2.1.2 Plating Cell

An optical view of the plating cell is shown in Figure 2.1.A. The cell was made of perspex with a screw in the side for tightening the specimen (dark zone) when immersed in the plating solution.

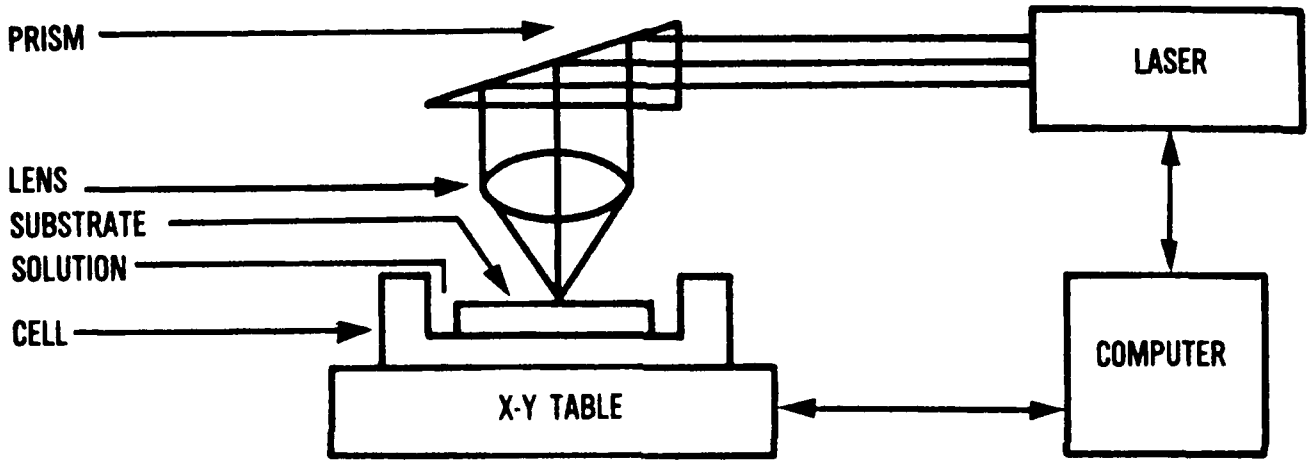

Fig. 2.1
SCHEMATIC VIEW OF THE EXPERIMENTAL SET UP FOR LASER PLATING PROCEDURE

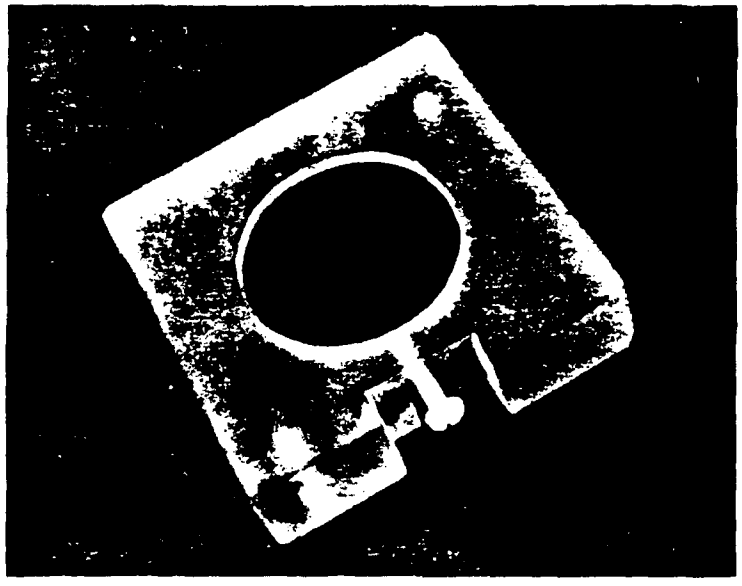

Fig. 2.1 A
OPTICAL VIEW OF THE PLATING CELL WITH A SUPERCONDUCTOR CERAMIC SPECIMEN IMMERSED IN THE MIDDLE OF THE CELL (DARK ZONE).

2.2 Experimental Procedure

2.2.1 Materials

2.2.1.1 Superconductive Ceramic Specimen

Specimens were prepared from Y BA_2 Cu_3 O_7 ceramic pellets. The pellets were prepared in a conventional way, i.e., burning premixed y_2o_3, $BaCO_3$ and CuO powders in air to 950°C for 12 hours. Grinding the burned compound and pressing the powder into 1.25 cm diameter pellets at R.T. up to 20,000 pounds and subsequently sinter the pellets in O_2 at 950°C for six hours [8].

Figure 2.1.B shows the relationship between the resistance of superconductor Y Ba_2 Cu_3 O_7 ceramic material on temperature. The transition temperature was found to be at 90°K below of which the material was superconductor.

2.2.1.2 Electroplating Gold Solution

Specimens made of Y Ba_2 Bu_3 O $_7$ superconductor materials are sensitive to the presence of water [5,6] as far as their chemical stability is concerned.

Therefore in this study nonaqueous plating solutions were used. Gold electroplating solution was prepared by dissolving 1 gr of $HAuCl_4$ salt in 50 cc dehydrated ethanol. The solutions were commercially available.

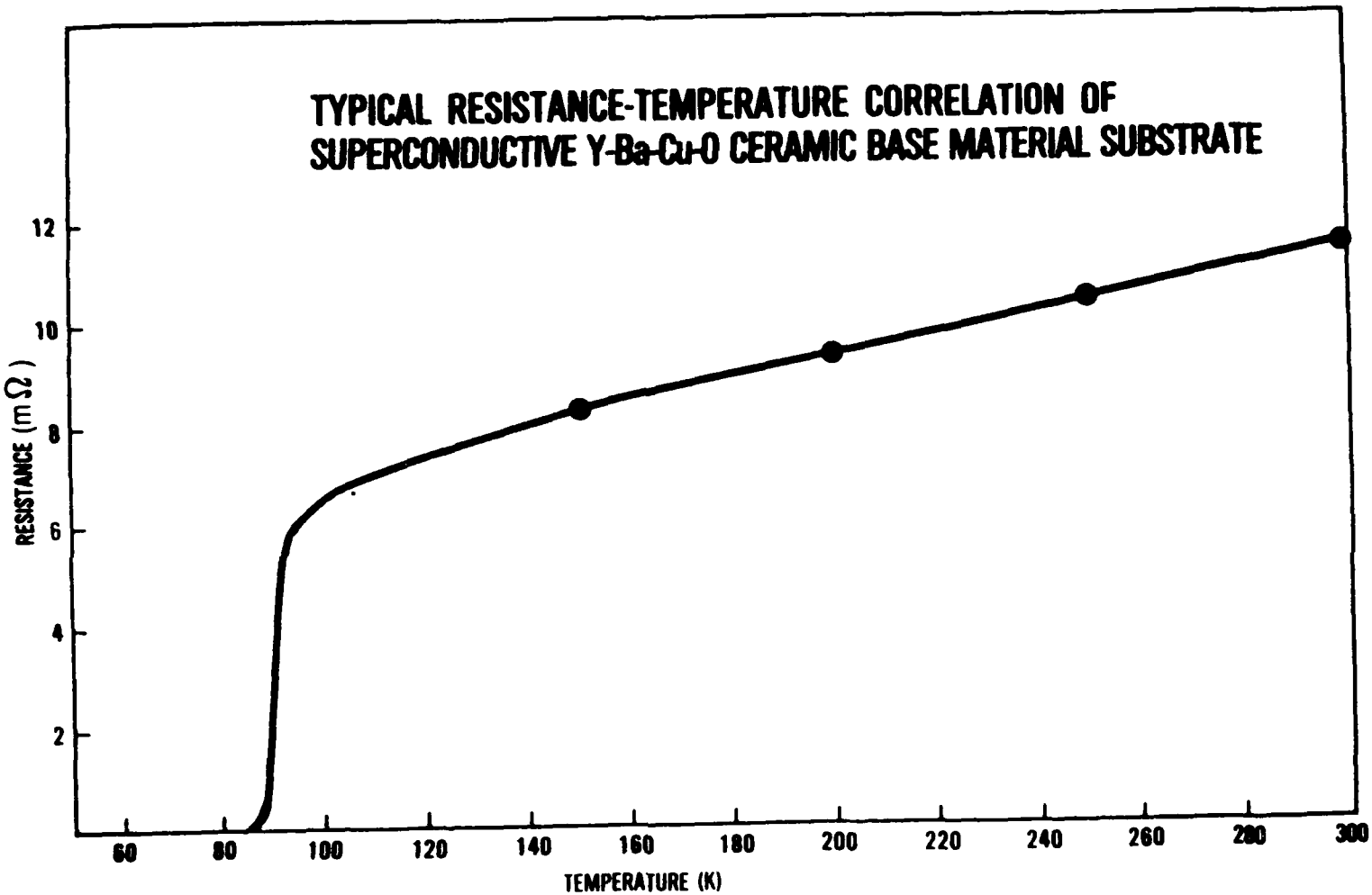

Fig. 2.1 B
RESISTANCE DEPENDANCE OF SUPERCONDUCTOR Y-Ba-Cu-O BASE CERAMIC MATERIAL ON TEMPERATURE. TRANSITION TEMPERATURE Tc WAS FOUND AT 90°K

2.2.2 Laser Plating Procedure

2.2.2.1 Laser Conditions

Laser irradiation conditions for gold plating were as follows:

Laser Energy: 1.0 - 3.0 mj/pulse

Laser Wavelength: 532mm

Laser Repetition Rate: 5 - 7 Hz.

Laser Beam Overlap: 95% - 50%

Laser Number of Pulses/Site: 1.0 - 1000

2.2.2.2 Deposition Processes

The procedure through which laser induced gold deposition from an electroplating solution onto a ceramic materials specimen is outlined in the following manner:

1. Set up laser irradiation conditions.
2. Alignment of laser beam through the various optics onto the specimen surface.
3. Preparation of electroplating gold solution 20g $HAuCl_4$ in 1000 cc dehydrated ethanol.
4. Preparation superconductive ceramic material specimen of Y_1 Ba_2 Cu_3 O_7.
5. Immersion of specimen into the plating solution.
6. Select the computer to control the laser irradiation procedures as well as to synchronize the X-Y table movements.
7. Operate the laser to get deposited gold at predetermined location on the specimen surface.
8. Stop laser irradiation when the process is completed.

9. Clean the specimen in dehydrated ethanol with ultrasonic cleaner.

10. Put the specimen in a vacuum to evaporate residues.

2.2.3 Deposit Observation and Characterization

Laser gold deposit pads produced on the superconductive ceramic materials specimen of Y-Ba-Cu-O, 1:2:3 base compound were examined by various techniques such as optical microscopy, scanning microscopy, auger electron spectroscopy (AES), electron spectroscopy of chemical analysis (ESCA). Also electrical measurements were carried out as to the resistance and contact resistance of the deposit pads on the ceramic substrate.

2.2.3.1 Optical and SEM Observation

Various types of optical microscopes were used for characterizing gold pads appearance on superconductive ceramic substrates. Surface views of the gold deposits produced via pulse laser irradiation under various conditions are given and described herein in paragraph 3.2.1.

Scanning electron microscopy (SEM) was used very effectively in characterizing gold deposit pads morphology, structure and composition. In this study the scanning electron microscope (SEM) was operated in various modes obtaining secondary electron images, backscattering electron images as well as making use of EDAX system getting x-ray analysis profile characteristics of the elements present. SEM micrographs either of secondary electron image or backscattered electron image are given and shown in paragraph 3.2.2.

2.2.3.2 AES and ESCA Analysis

A. AES

Auger electron spectroscopy (AES) is a nondestructive technique for surface chemical analysis with particularly small depth resolution and hence is well suitable to study solid surfaces. Auger electron spectroscopy (AES) is achieved by making an energy analysis of electrons ejected from a solid. It is an electron excited technique which is initiated by bobarding the material with a beam of electrons. Typical electron beam energy is 5 kev and typical beam diameter 5μm to 25 μm. Limit of detectability is on the order of 0.1% atomic concentration. Figure 2.1.C describes schematically AES processes involving bombarding materials surface with a beam of electrons which can ionize one of the electron levels such as the K level. An electron from n level, say, can drop down to fill the vacant K shell. While doing that the electron leaving n shell can transfer its energy to electron at n energy level which can then have enough energy to be ejected from the solid surface. This electron will then have an energy related to n and K level. Measuring the escaped electron energy will make it possible to analyze and identify the elements in the materials surface. The process described can be defined as the KMN transition.

AES surface analysis was found very effective in identifying the presence of various elements at laser irradiated zones on the superconductive ceramic material as shown herein in paragraph 3.2.3.

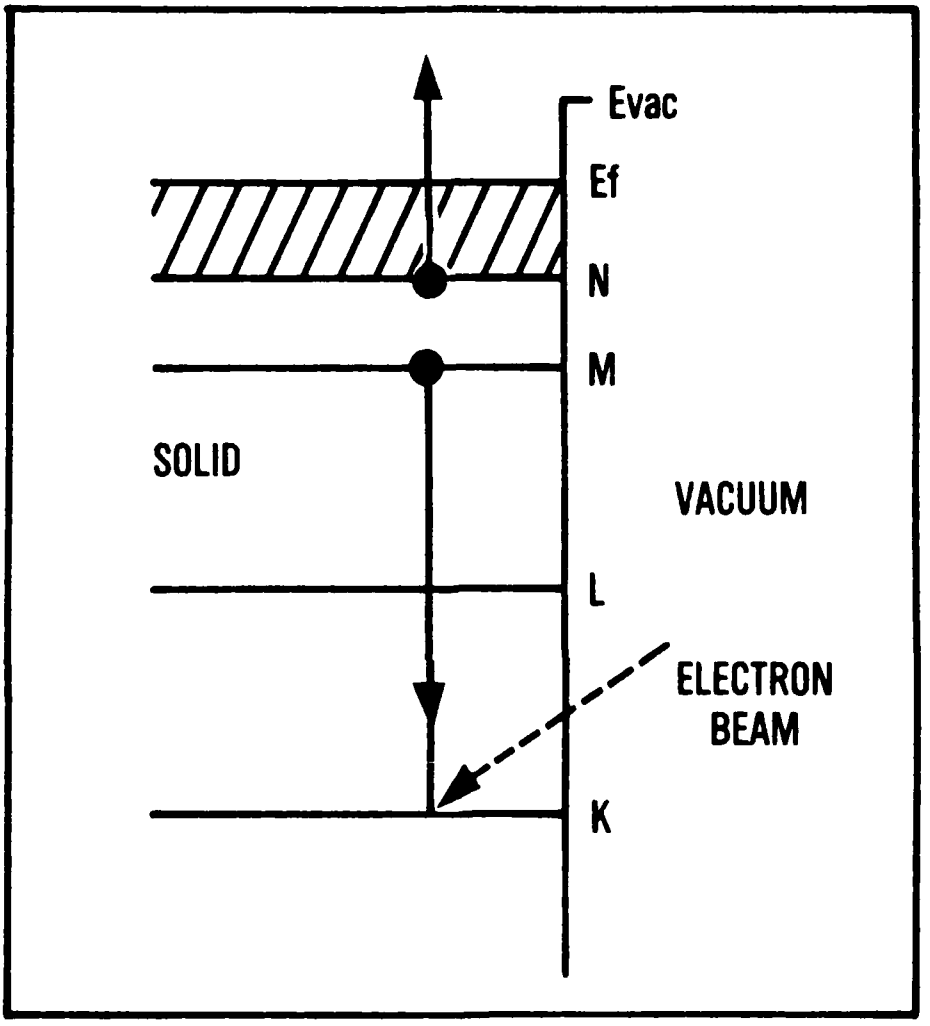

Fig. 2.1 C
SCHEMATIC AES ENERGY LEVELS DIAGRAM

B. ESCA

Electron spectroscopy for chemical analysis is a very powerful technique in surface analyses studies. ESCA processes involved the bombardment of x-ray on to the surface of the sample. Absorption of the x-rays results in prompt emission of photoelectrons from atomic orbitals whose binding energy is less than the x-ray energy. X-ray energy will have to be absorbed at such level so it can remove an electrons from the atom that adsorbed the x-ray. Namely x-ray energy should be higher than the binding energy E_b of the electron. Actually that is the ionization potential. Energy in excess of E_b appears as the kinetic energy of the electron when it leaves the atom. It is that energy which is being measured. The x-ray energy minus the kinetic energy will give the binding energy. In commercial instrument the binding energy is calculated and being displayed. ESCA is a very sensitive technique because the photoelectrons have to leave the surface without loosing their energy. Therefore only the electrons that originate near the surface would be able to escape from the sample surface without loosing energy. Escape characteristic depth of photoelectrons will be in the range of 10-100Å. Therefore effective ESCA analysis would be in depth of 10Å-100Å of the surface examined. ESCA technique was found very beneficial in identifying various elements and compounds on and around gold deposit pads formed via pulse laser irradiation on superconductive ceramic materials.

2.2.3.3 Electrical and Contact Resistance Measurements

Electrical measurements of high Tc superconductive substrate material as well as of laser gold deposited lines or the substrate surface were conducted by making use of two point probes and of four point probe procedures [18].

A. Two point probes resistance measurement procedure involved the use of two probes touching the material surface at a given distance between the two probes. Furthermore the two probes were connected to a current supply and a voltmeter measuring the voltage drop while changing the current, or in other words producing I-V curves. The slop of the I-V curve indicates the resistance value of the measured substance.

Superconductive specimen bulk material was evaluated for its resistance by two point probes as well as the gold deposited lines on the superconductor specimen surface. The probes used in this study were gold plated crown probes. Crown probes consist of 9 pins with a diameter of .1mm each on a 1 mm diameter surface. Also used were probes with rounded tips so as not to penetrate through the gold deposit.

The crown probes were used for measuring conduct resistivity of the surface of the bulk material, while the rounded tip probes were used for measuring the conduct resistivity of the gold line.

B. The four point probe method of measurement was used to determine both the conduct resistivity of the bulk material and the contact resistance of the gold lines to the super conductive material. A schematic views of four point probes measurements are shown in

Figure 2.5. Current is supplied through the outer probes (No.1,4) while potential drop is measured between the inner probes (No.2,3). The probes are equally spaced. Fig 2.5.B demonstrates the procedure for measuring contact resistance of laser gold deposit pad on superconductor substrate specimen. The ratio between the potential drop and the current value will give resistance values. In this study the current was kept constant at 100 mA while the voltage difference was in the range of mV and less.

- Measuring contact resistance at low temperature range from R.T. to liquid helium temperature is shown schematical in Figure 2.6. The basic four point probes arrangement is shown in Figure 2.7.

In that system (Figure 2.7) the gold leads are connected to the gold pad either through an ultrasonic pressure bonding procedure or with the aid of Indium or silver. One can see that the current lead is connected to the gold pads as well as one of the voltage leads. There are two voltage leads connected to the superconductor surface for measuring voltage drop as function of temperature while constant current in the order of 1.0 mA, 10.0 mA or 100.0 mA is applied.

Based on the connection procedure shown in Figure 2.7 the contact resistance should be calculated as follows:

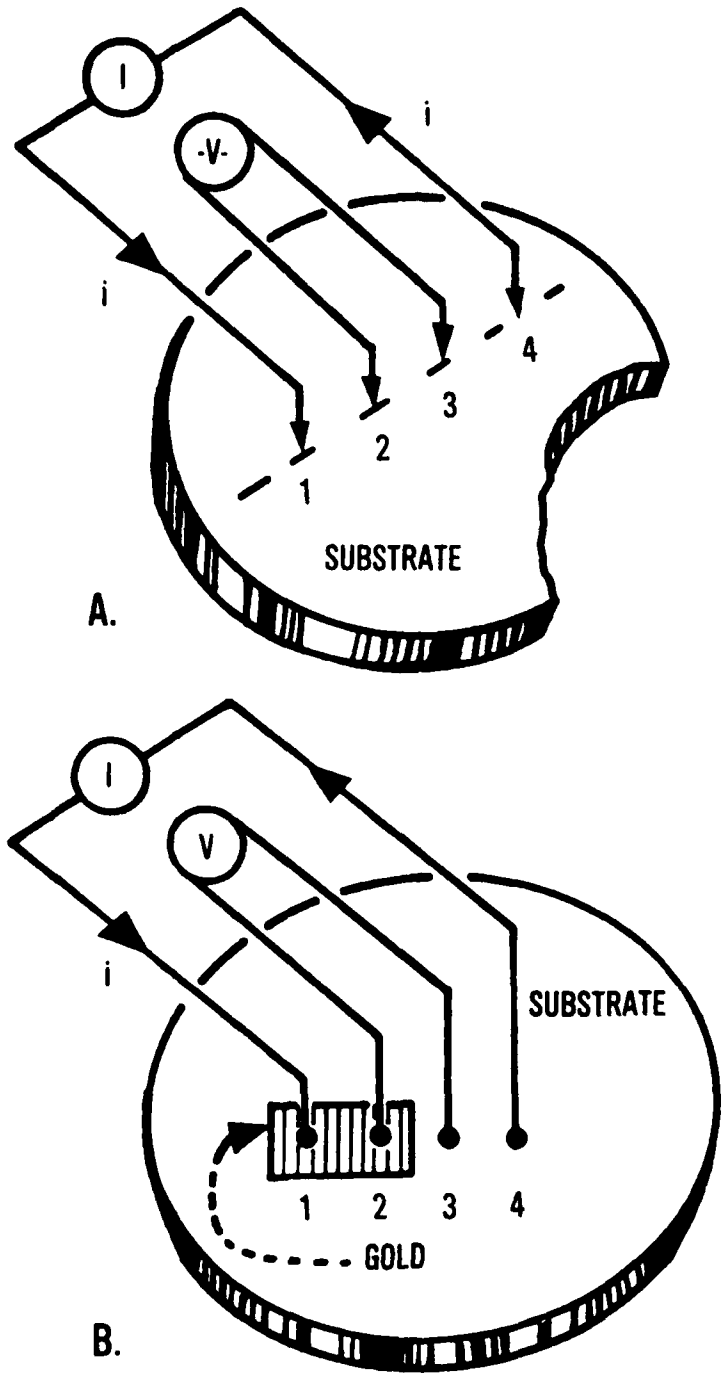

FIG 2.5: FOUR POINT PROBES ARRANGEMENT. PROBES NO. 1 AND 4 ARE THE CURRENT INPUT. PROBES 2, 3 MEASURE THE POTENTIAL DIFFERENCE, V, BETWEEN THEM. THE PROBES ARE EQUALLY SPACED.
A. MEASURING SUBSTRATE SPECIMEN MATERIAL
B. MEASURING GOLD DEPOSIT PADS ON THE SURFACE.

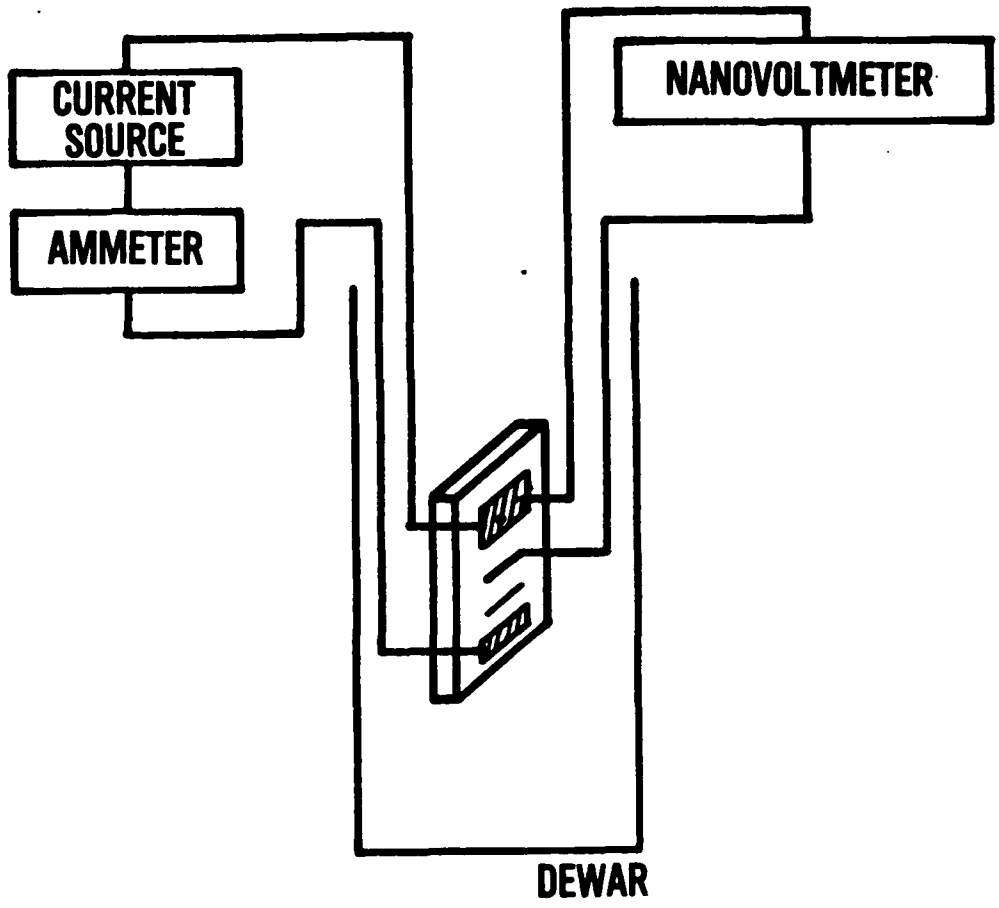

Fig. 2.6
SCHEMATIC VIEW OF THE SYSTEM USED FOR MEASURING CONTACT RESISTANCE OF GOLD PADS ON SUPERCONDUCTIVE CERAMIC MATERIAL AT LOW TEMPERATURES NAMELY FROM R.T. DOWN TO LIQUID HELIUM TEMPERATURE AROUND 4°K

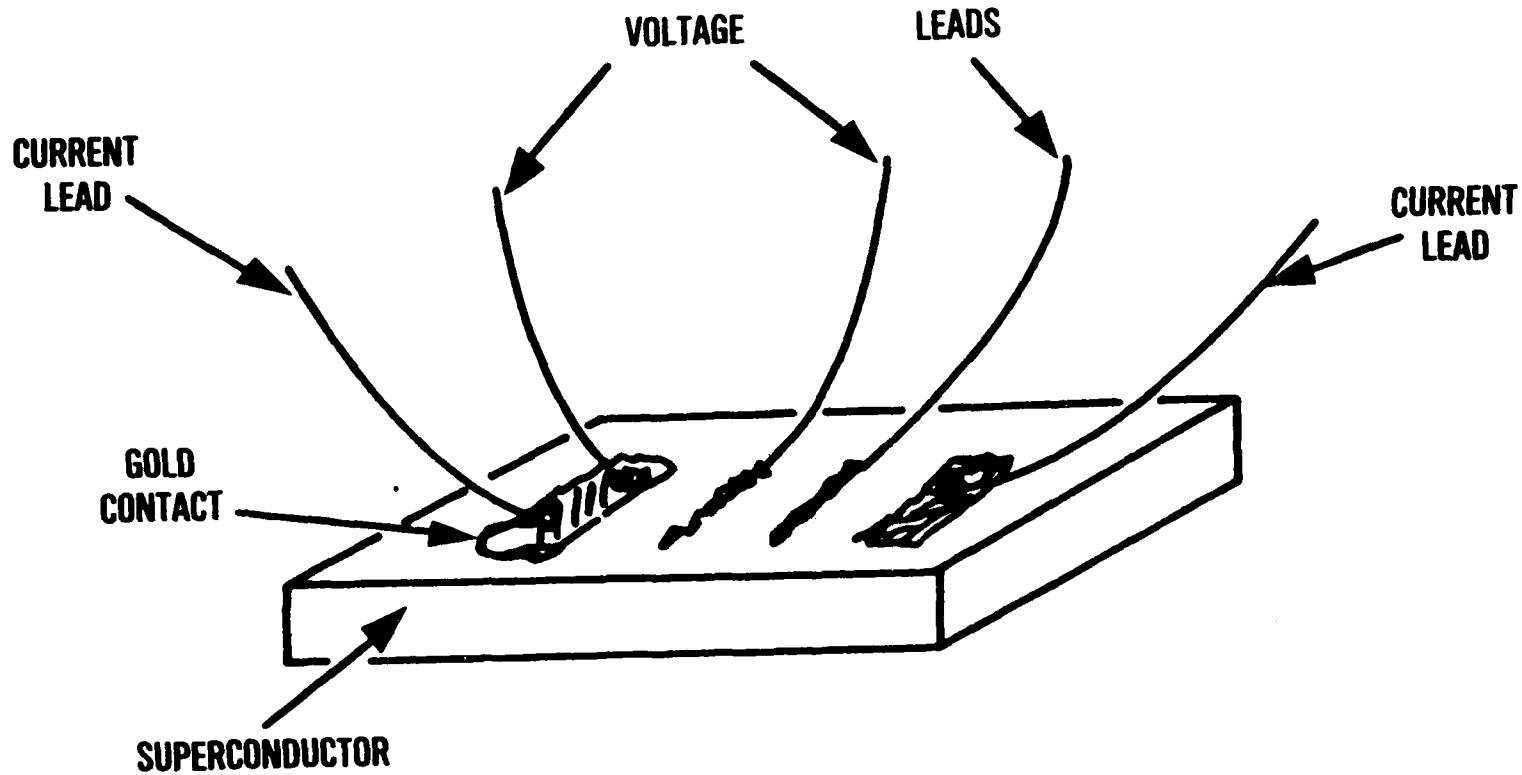

Fig. 2.7
SCHEMATIC VIEW OF VOLTAGE AND CURRENT PROCEDURE IN MEASURING CONTACT RESISTANCE AT LOW TEMPERATURES SYSTEM

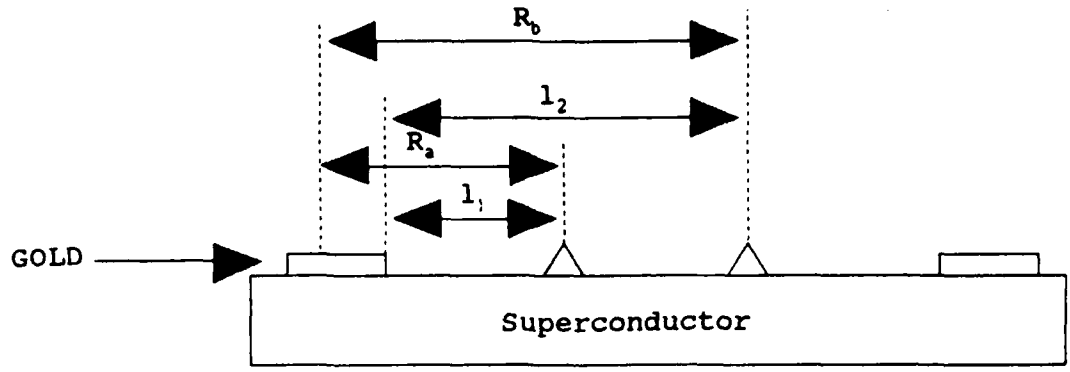

(1) $R_c + l_1 r_{sc} = R_a$

(2) $R_c + l_2 r_{sc} = R_b$

Solving (1) + (2) will eliminate r_{sc} and will give:

(3) $$R_c = \frac{l_2 R_a - l_1 R_b}{l_2 - l_1}$$

Where:

R_c = Contact Resistance

R_b, R_a = Resistance

$r_{sc} = \rho_{sc}/\text{Area}$

ρ_{sc} = Superconductor Resistivity

In these simple calculations it is assumed that the superconductor resistance r_{sc} is linear with distance. The values of R_b and R_a can be calculated by dividing the measured potential drops by the constant current imposed.

3.0 RESULTS AND DISCUSSIONS

This project aimed at studying for the first time the feasibility of direct, high speed gold plating via YAG pulsed laser irradiation on superconductor ceramic Y-Ba-Cu-O base material immersed in the plating solution. Substantial efforts were made in finding out the laser operational conditions to give either dots, lines or pads of laser gold deposits. These deposits were examined thereafter for their morphology, structure, composition and electrical properties, especially their resistance.

3.1 Laser Induced Gold Deposit Formation

The experimental conditions under which gold deposit of points and lines were produced via pulse laser irradiation are described in Table 3.1. The conditions under which gold deposit pads were formed in the sizes of 2mm x 5mm or 5mm x 5mm or in other sizes like 1mm x 1mm are described primarily in Table 3.2.

Experimental conditions of YAG pulse laser irradiation on superconductors Y-Ba-Cu-O ceramic base material immersed in gold methanol solution (Table 3.1 Sample A, Exp. I) resulted in damaging the substrate at the irradiated zones. That result could be attributed to high laser beam energy density above 2 mj/pulse. However, around the damage areas deposits of gold could be detected. In subsequent experiments the laser beam energy was reduced to 1.0 mj/pulse and the gold plating solution was changed to gold ethanol (Table 3.1, Sample A, Exp. II, Lines 1,2,3,4). Under these conditions no gold deposit was detected on the ceramic substrate. Thereafter

TABLE 3.1

FORMATION OF GOLD DEPOSIT LINES FROM ELECTORPLATING SOLUTIONS
ON SUPERCONDUCTIVE Y-Ba-Cu-O CERAMIC MATERIALS
UNDER VARIOUS LASER IRRADIATION CONDITIONS

ELECTROPLATING SOLUTION: 1gr $HAuCl_4$ In 50ml Methanol

LASER IRRADIATION CONDITIONS YAG LASER: Pulse irradiation beam diameter 1mm, R.R. = 5Hz
WAVELENGTH: 532nm, pulse duration, 15ns

SAMPLE NUMBER	EXPERIMENT NUMBER	LINE NUMBER	BEAM MOVEMENT ALONG LINE [μm]	BEAM OVERLAP (%)	NUMBER OF PULSES PER SITE	NUMBER OF SITES	NUMBER OF TOTAL PULSES	LASER BEAM ENERGY mj/pulse
A	EXP I	1	500	50	100	10	1000	1
		2	---	--	100	10	1000	3
		3	100	90	100	10	1000	2
		4	500	50	1000	5	5000	2
		5	500	50	1000	5	5000	3
		6	0.5	99.5	1	4000	4000	3

TABLE 3.1 (CONT)

FORMATION OF GOLD DEPOSIT LINES FROM ELECTORPLATING SOLUTIONS
ON SUPERCONDUCTIVE Y-Ba-Cu-O CERAMIC MATERIALS
UNDER VARIOUS LASER IRRADIATION CONDITIONS

ELECTROPLATING SOLUTION: 1gr $HAuCl_4$ In 200ml Dehydrated Ethanol

LASER IRRADIATION CONDITIONS YAG LASER: Pulse irradiation beam diameter 1mm, R.R. = 5Hz
WAVELENGTH: 532nm, pulse duration, 15ns

SAMPLE NUMBER	EXPERIMENT NUMBER	LINE NUMBER	BEAM MOVEMENT ALONG LINE [μm]	BEAM OVERLAP (%)	NUMBER OF PULSES PER SITE	NUMBER OF SITES	NUMBER OF TOTAL PULSES	LASER BEAM ENERGY mj/pulse
A	EXP II	1	---	---	5	7	35	1
		2	---	---	20	7	140	1
		3	---	---	100	6	600	1
		4	---	---	200	---	---	1

TABLE 3.1 (CONT)

FORMATION OF GOLD DEPOSIT LINES FROM ELECTORPLATING SOLUTIONS
ON SUPERCONDUCTIVE Y-Ba-Cu-O CERAMIC MATERIALS
UNDER VARIOUS LASER IRRADIATION CONDITIONS

ELECTROPLATING SOLUTION: 1gr $HAuCl_4$ In 50ml Dehydrated Ethanol

LASER IRRADIATION CONDITIONS YAG LASER: Pulse irradiation beam diameter 1mm, R.R. = 5Hz
WAVELENGTH: 532nm, pulse duration, 15ns

SAMPLE NUMBER	EXPERIMENT NUMBER	LINE NUMBER	BEAM MOVEMENT ALONG LINE [μm]	BEAM OVERLAP (%)	NUMBER OF PULSES PER SITE	NUMBER OF SITES	NUMBER OF TOTAL PULSES	LASER BEAM ENERGY mj/pulse
A	EXP III	1	500	50	100	4	400	1.5
		2	500	50	1000	4	4000	1.5
		3	500	50	1000	4	4000	2.0
		4	500	50	100	4	400	2.0
		5	5	99.5	1	1000	1000	2.0

TABLE 3.1 (CONT)

FORMATION OF GOLD DEPOSIT LINES FROM ELECTORPLATING SOLUTIONS
ON SUPERCONDUCTIVE Y-BA-CU-O CERAMIC MATERIALS
UNDER VARIOUS LASER IRRADIATION CONDITIONS

ELECTROPLATING SOLUTION: 1gr $HAuCl_4$ In 50ml Dehydrated Ethanol

LASER IRRADIATION CONDITIONS YAG LASER: Pulse irradiation beam diameter 1mm, R.R. = 5Hz
WAVELENGTH: 532nm, pulse duration, 15ns

SAMPLE NUMBER	EXPERIMENT NUMBER	LINE NUMBER	BEAM MOVEMENT ALONG LINE [μm]	BEAM OVERLAP (%)	NUMBER OF PULSES PER SITE	NUMBER OF SITES	NUMBER OF TOTAL PULSES	LASER BEAM ENERGY mj/pulse
A	EXP IV	1	50	95	100	20	2000	2.0
		2	50	95	500	20	10000	2.0
		3	50	95	200	20	4000	2.0
		4	250	75	2000	6	12000	2.0
		5	50	95	300	10	3000	2.0

TABLE 3.1 (CONT)

FORMATION OF GOLD DEPOSIT LINES FROM ELECTORPLATING SOLUTIONS
ON SUPERCONDUCTIVE Y-BA-CU-O CERAMIC MATERIALS
UNDER VARIOUS LASER IRRADIATION CONDITIONS

ELECTROPLATING SOLUTION: 1gr $HAuCl_4$ In 50ml Dehydrated Ethanol

LASER IRRADIATION CONDITIONS YAG LASER: Pulse irradiation beam diameter 1mm, R.R. = 5Hz
WAVELENGTH: 532nm, pulse duration, 15ns

SAMPLE NUMBER	EXPERIMENT NUMBER	LINE NUMBER	BEAM MOVEMENT ALONG LINE [μm]	BEAM OVERLAP (%)	NUMBER OF PULSES PER SITE	NUMBER OF SITES	NUMBER OF TOTAL PULSES	LASER BEAM ENERGY mj/pulse
B	EXP V	1A	50	95	1	40	40	2.0
		1B	50	95	1	40	40	2.0
		2A	50	95	10	40	400	2.0
		2B	50	95	10	40	400	2.0
		3A	50	95	100	40	4000	2.0
		3B	50	95	100	40	4000	2.0
		4A	50	95	200	40	8000	2.0
		4B	50	95	200	40	8000	2.0

TABLE 3.2

FORMATION OF GOLD DEPOSIT ZONES ON SUPERCONDUCTIVE Y-Ba-Cu-O CERAMIC MATERIALS UNDER VARIOUS LASER IRRADIATION CONDITIONS

ELECTROPLATING SOLUTION: 1gr $HAuCl_4$ In 50ml Dehydrated Ethanol

LASER IRRADIATION CONDITIONS YAG LASER: Pulse irradiation, beam diameter 1mm, R.R. = 5 - 6 Hz
WAVELENGTH: 532nm, pulse duration, 15ns

Sample Number	Experiment Number	Set Number	Zone Number	Beam Movement Along Line [μm]	Beam Overlap (%)	Pulses Per Site	Number of Sites	Beam Movement Cross Line [μ]	Beam Overlap (%)	Pulses Per Site	Number of Sites	Number of Total Pulses	Laser Beam Energy mj/pulse
E	VII	-	1	50	95	20	100	500	50	20	6	12000	1.3
			2	50	95	30	100	500	50	30	6	18000	1.3
C	VI	-	1	50	95	20	100	500	50	20	6	12000	2.0
			2	50	95	20	100	500	50	20	6	12000	2.0
			3	50	95	20	100	500	50	20	6	12000	2.0
D	VIII	A	1	50	95	30	40	250	75	30	2	2400	1.3
			2	50	95	30	40	250	75	30	2	2400	1.3
			3	50	95	30	40	250	75	30	2	2400	1.3
			4	50	95	30	40	100	90	30	2	2400	1.3
		B	1	50	95	40	40	100	90	40	2	3200	1.3
			2	50	95	40	40	100	90	40	2	3200	1.3
			3	50	95	40	40	100	90	40	2	3200	1.3
			4	50	95	40	40	100	90	40	2	3200	1.3

TABLE 3.2 (CONT)

FORMATION OF GOLD DEPOSIT ZONES ON SUPERCONDUCTIVE Y-Ba-Cu-O CERAMIC MATERIALS UNDER VARIOUS LASER IRRADIATION CONDITIONS

ELECTROPLATING SOLUTION: 1gr $HAuCl_4$ In 50ml Dehydrated Ethanol

LASER IRRADIATION CONDITIONS YAG LASER: Pulse irradiation, beam diameter 1mm, R.R. = 5 - 6 Hz
WAVELENGTH: 532nm, pulse duration, 15ns

SAMPLE NUMBER	EXPERIMENT NUMBER	SET NUMBER	ZONE NUMBER	BEAM MOVEMENT ALONG LINE [μm]	BEAM OVERLAP (%)	PULSES PER SITE	NUMBER OF SITES	BEAM MOVEMENT CROSS LINE [μ]	BEAM OVERLAP (%)	PULSES PER SITE	NUMBER OF SITES	NUMBER OF TOTAL PULSES	LASER BEAM ENERGY mj/pulse
D	VIII	C	1	50	95	50	40	100	90	50	2	4000	1.3
			2	50	95	50	40	100	90	50	2	4000	1.3
			3	50	95	50	40	100	90	50	2	4000	1.3
			4	50	95	50	40	100	90	50	2	4000	1.3
E	IX	A	1	50	95	30	50	250	75	30	2	3000	1.5
			2	50	95	30	50	250	75	30	2	3000	1.5
			3	50	95	30	50	250	75	30	2	3000	1.5
			4	50	95	30	50	250	75	30	2	3000	1.5
		B	1	50	95	30	10	250	75	30	2	600	1.5
			2	50	95	30	10	250	75	30	2	600	1.5
			3	50	95	30	10	250	75	30	2	600	1.5
			4	50	95	30	10	250	75	30	2	600	1.5

TABLE 3.2 (CONT)

FORMATION OF GOLD DEPOSIT ZONES ON SUPERCONDUCTIVE Y-Ba-Cu-O CERAMIC MATERIALS UNDER VARIOUS LASER IRRADIATION CONDITIONS

ELECTROPLATING SOLUTION: 1gr $HAuCl_4$ In 50ml Dehydrated Ethanol

LASER IRRADIATION CONDITIONS YAG LASER: Pulse irradiation, beam diameter 1mm, R.R. = 5 - 6 Hz
WAVELENGTH: 532nm, pulse duration, 15ns

SAMPLE NUMBER	EXPERIMENT NUMBER	SET NUMBER	ZONE NUMBER	BEAM MOVEMENT ALONG LINE [μm]	BEAM OVERLAP (%)	PULSES PER SITE	NUMBER OF SITES	BEAM MOVEMENT CROSS LINE [μ]	BEAM OVERLAP (%)	PULSES PER SITE	NUMBER OF SITES	NUMBER OF TOTAL PULSES	LASER BEAM ENERGY mj/pulse
E	IX	C	1	50	95	50	50	250	75	50	2	5000	1.5
			2	50	95	50	50	250	75	50	2	5000	1.5
			3	50	95	50	50	250	75	50	2	5000	1.5
			4	50	95	50	50	250	75	50	2	5000	1.5
		D	1	50	95	50	10	250	75	50	2	1000	1.5
			2	50	95	50	10	250	75	50	2	1000	1.5
			3	50	95	50	10	250	75	50	2	1000	1.5
			4	50	95	50	10	250	75	50	2	1000	1.5
F	X		1	50	95	30	100	250	75	50	20	6000	1.5
			2	50	95	5	100	250	75	5	20	10000	1.5

laser beam energy was selected between 1.3 to 2.0 mj/pulse while beam diameter at the irradiated area was 1mm.

Laser beam step movements (or rather movement of the X-Y table) were from 5 μm steps through 50 μm steps up to 500 μm steps (see tables 3.1, 3.2). These sizes of steps actually resulted in beam overlapping form 99.5% to 90% up to 50% and thus forming probably a thicker and denser gold deposits at the irradiated zones.

An important factor involved in the processes of laser deposition was the number of laser irradiation pulses per site namely the number of pulses at each step of movement. In Table 3.1 it can be seen that the number of pulses ran from 1.0 pulse per site, through 100, 200, 500 up to 2,000 pulses/site. It was found that values of 20 to 40 pulses per site at overlapping of 95% gave substantial amount of gold deposit to be clearly detected by naked eyes (see Table 3.2). Gold deposition via pulse laser irradiation on superconductor ceramic material should be continued to get reliable correlations such as the dependence of gold deposit thickness and its electrical properties on laser number of pulses at given energy; on laser energy; on laser overlapping degree; and on laser wavelength. Also the use of various nonaqueous gold plating solutions should be examined.

3.2 Deposit Morphology and Structure

Laser gold deposit morphology and structure was examined by making use of optical and scanning electron microscopy.

3.2.1 Optical Microscopy

Typical optical views of gold deposits on superconductor Y-Ba-Cu-O base ceramic material are shown in Figures 3.1-3.5.

Figure 3.1 shows the appearance of irradiated surface along six lines. Damage in forms of holes in the ceramic surface at the laser irradiated zones can be seen very clearly (Figure 3-1, Table 3.1, Sample A, Exp, I). However around the holes one can observe some gold deposits. It might be pointed out that the damage was caused by high energy density of the laser beam namely above 2 mj/pulse. Under lower beam energy in the value of 1.5 mj/pulse to 2.0 mj/pulse one could obtain very clear gold deposits without introducing damage in the superconductive ceramic substrate as shown in Figure 3.2. Deposit lines were produced under various irradiation conditions (See Table 3-1, Sample A, Exp. III) and that is reflected in their appearance in Figure 3.2.A. Figure 3.2.B. simply shows Line No. 3 in magnification. No damage to the substrate was observed. Furthermore, gold deposits followed the rough and porous morphology of the substrate itself.

Figures 3.3 and 3.4 show typical gold deposit pads 5mm x 3mm formed on Sample B (Figure 3.3) and on Sample C (Figure 3.4). It might be seen very clearly that gold deposit processes were followed the morphology of the ceramic substrate (Figure 3.3.A, 3.3.B). Furthermore, the presence of cracks and pores (Figure 3.3.A) did not prevent to get what seemed to be good gold deposits (Figure 3.3.B, 3.3.C).

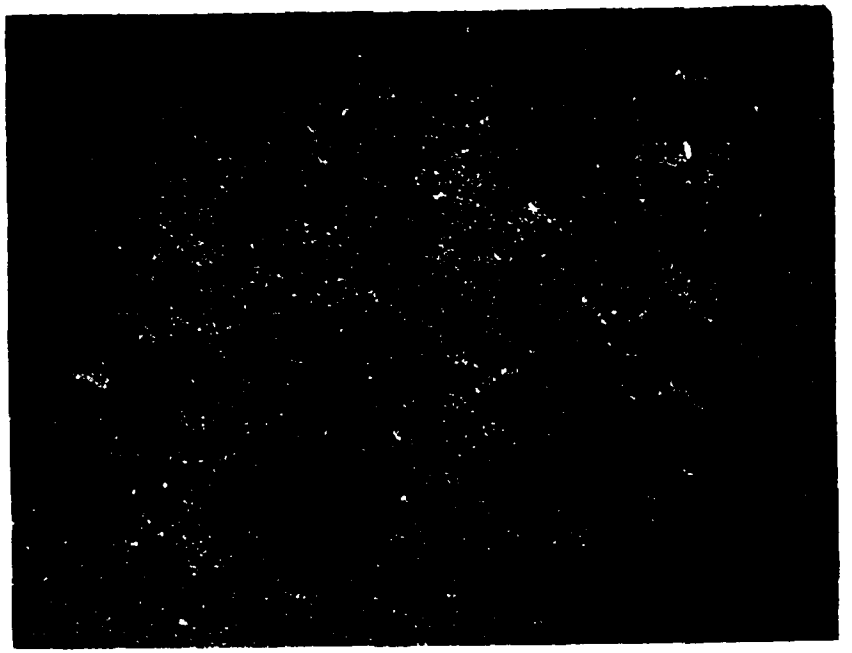

LINE No. 6 5 4 3 2 1

Fig. 3.1
OPTICAL MICROSCOPE VIEW OF SUPERCONDUCTOR SPECIMEN AFTER BEING LASER IRRADIATED TO FORM GOLD LINES. [SEE TABLE 3.1 , SAMPLE A , EXP. I] NOTICE HOLES FORMATION WITH GOLD DEPOSIT AROUND THEM

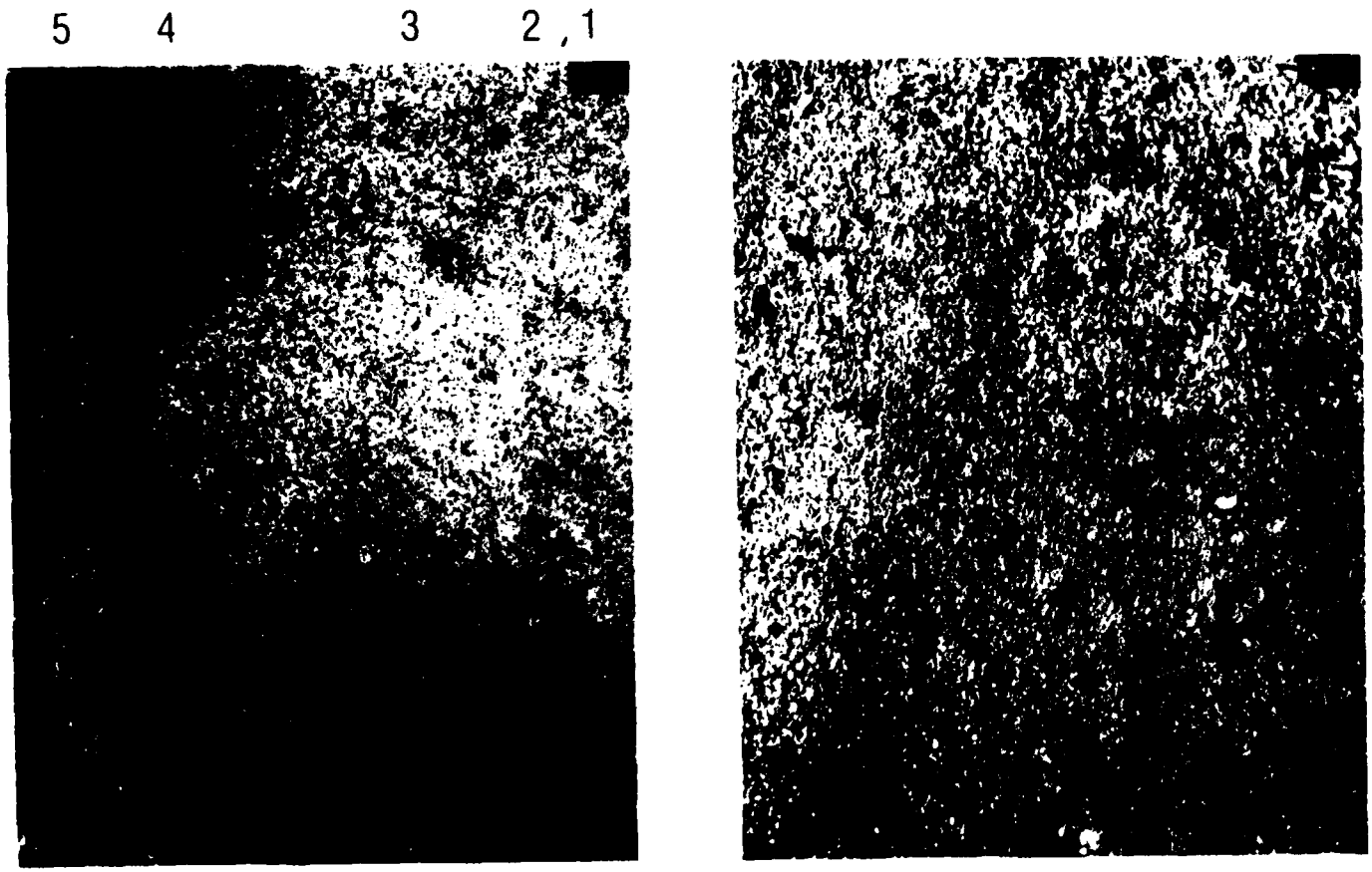

Fig. 3.2
OPTICAL MICROSCOPY VIEW OF GOLD DEPOSIT LINES PRODUCED VIA LASER PULSE IRRADIATION [SEE TABLE 3.1 SAMPLE A , EXP. III] A. LOW MAG OF GOLD LINES 1, 2, 3, 4, 5
B. HIGH MAG OF LINE 3

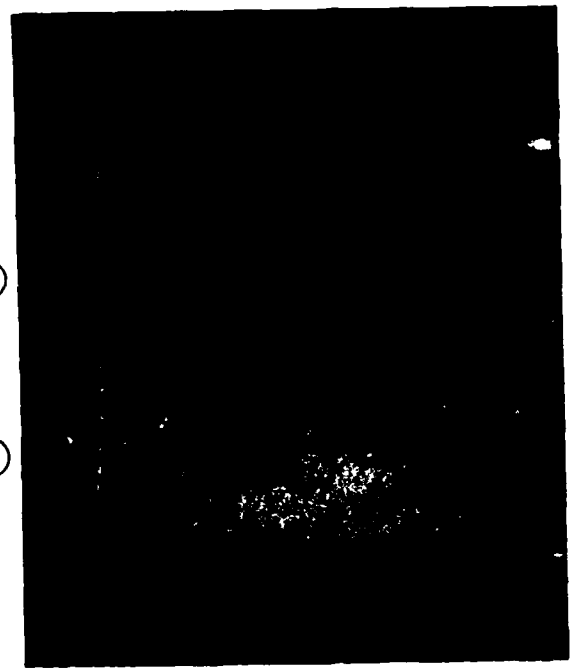

A

B

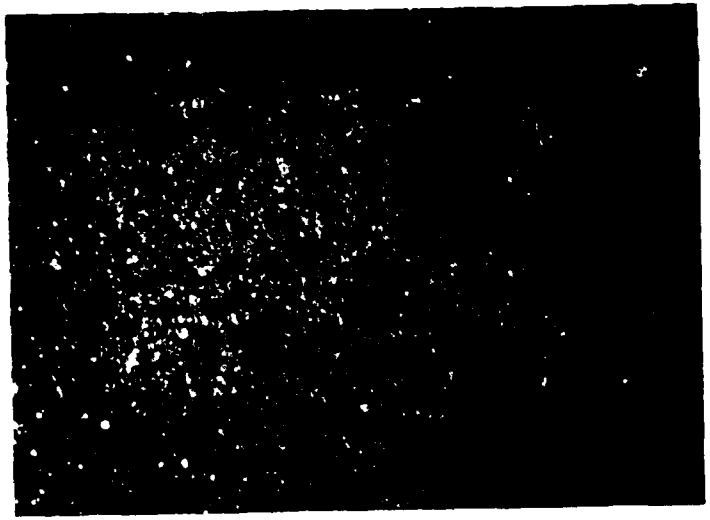

C

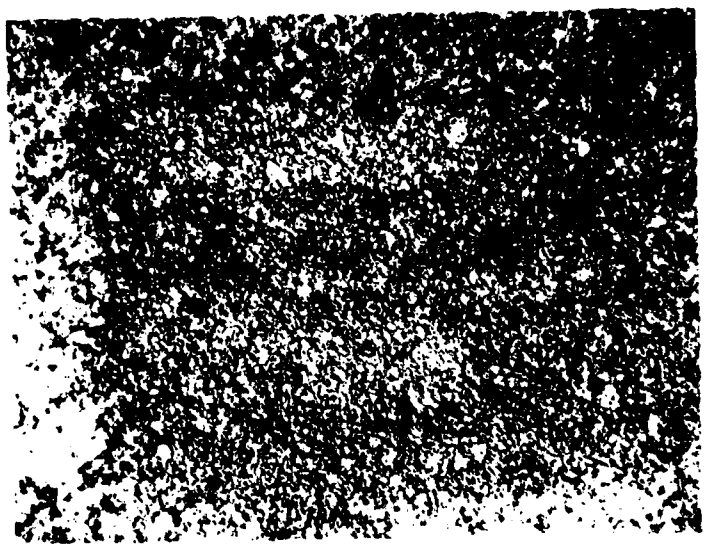

Fig. 3.3
OPTICAL MICROSCOPE VIEW OF GOLD DEPOSIT PADS FORMED VIA LASER IRRADIATION ON SUPERCONDUCTIVE SPECIMEN. [SEE TABLE 3.2, SAMPLE B, EXP. VII]
A. LOW MAG OF GOLD PADS No. 1 AND No. 2 ON SUPERCONDUCTIVE CERAMIC SUBSTRATE B. ENLARGEMENT OF GOLD PAD No. 2 C. ENLARGEMENT OF GOLD PAD No. 1

A

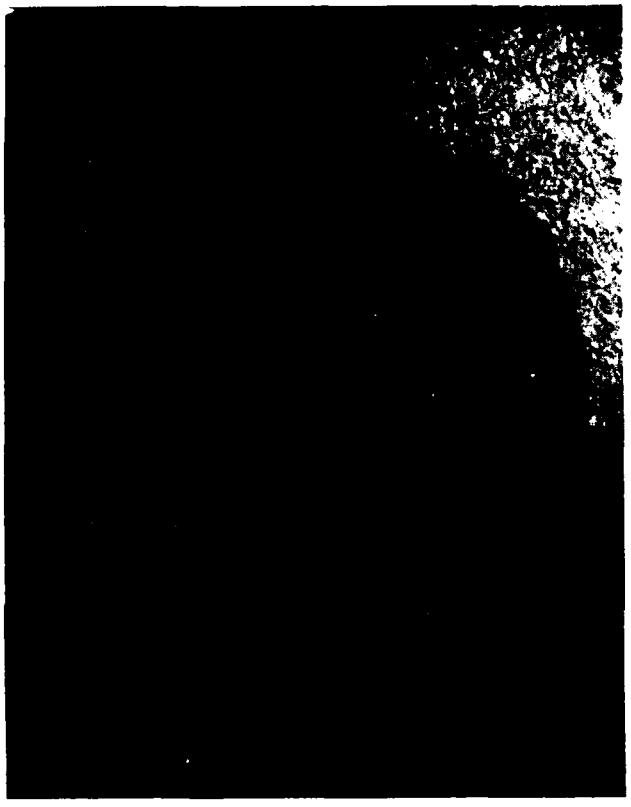

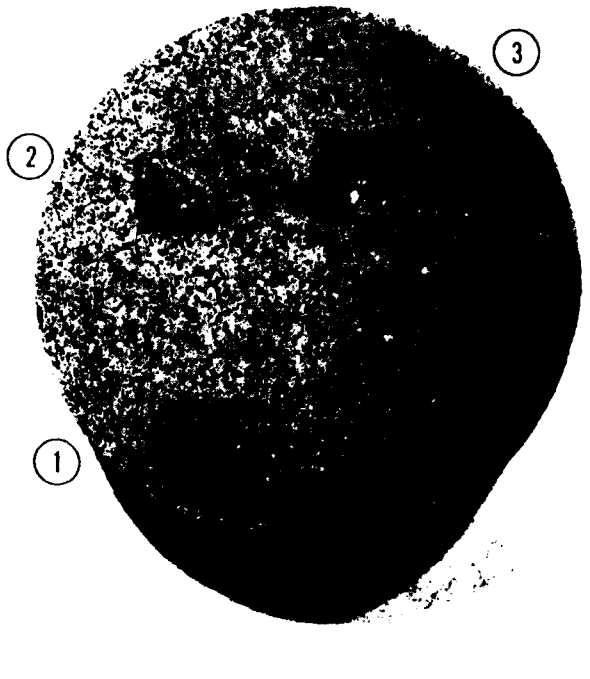

B

Fig. 3.4
OPTICAL VIEW OF GOLD PADS FORMED VIA PULSE LASER IRRADIATION ON SUPERCONDUCTIVE CERAMIC SUBSTRATE [SEE TABLE 3.2 , SAMPLE C , EXP. VI] A. COLOR PICTURE OF GOLD PADS No. 1, 2, 3 B. BLACK AND WHITE PICTURE OF PADS 1, 2, 3

Typical sets of gold deposit pads especially for measuring contact resistance values are shown in Figure 3.5. It might be noted that the pads shown in Figure 3.5.B appeared thicker and denser compared to the pads shown in Figure 3.5.A. The difference could be due to the fact that the thicker pads (in Figure 3.5.B) were formed at laser irradiation of 50 pulses/site compared to 30 pulses/site. (See Table 3.2, Sample E, Exp. IX).

The optical microscope was a very useful device for initial and quick observation of gold deposit spots, lines and pads of various sizes. Also it give information regarding possible surface damage under the various conditions of laser irradiation.

3.2.2 Scanning Electron Microscopy

Detailed view of gold deposit surface morphology and structure was obtained by SEM through backscatted and secondary electron images as shown in Figure 3.6 through Figure 3.13.

Typical SEM view of irradiated area where damage was observed (Figure 3.1) is shown in Figure 3.6. The damage was characterized by holes formation in the ceramic surface (dark zone in Figure 3.6). Around the hole one could observe the detailed morphology of the substrate itself (Table 3.1, Sample A, Exp. I, Line 4). Figure 3.7 shows the same gold lines as shown by optical microscopy in Figure 3.2 A backscattered electron image indicated the presence of gold lines as shown clearly in Figure 3.7.A (Bright Zones). In nonirradiated zones no gold was deposited (dark areas in Figure 3.7.A.). Furthermore, a secondary electron image of the zone shown in 3.7.A did not indicate

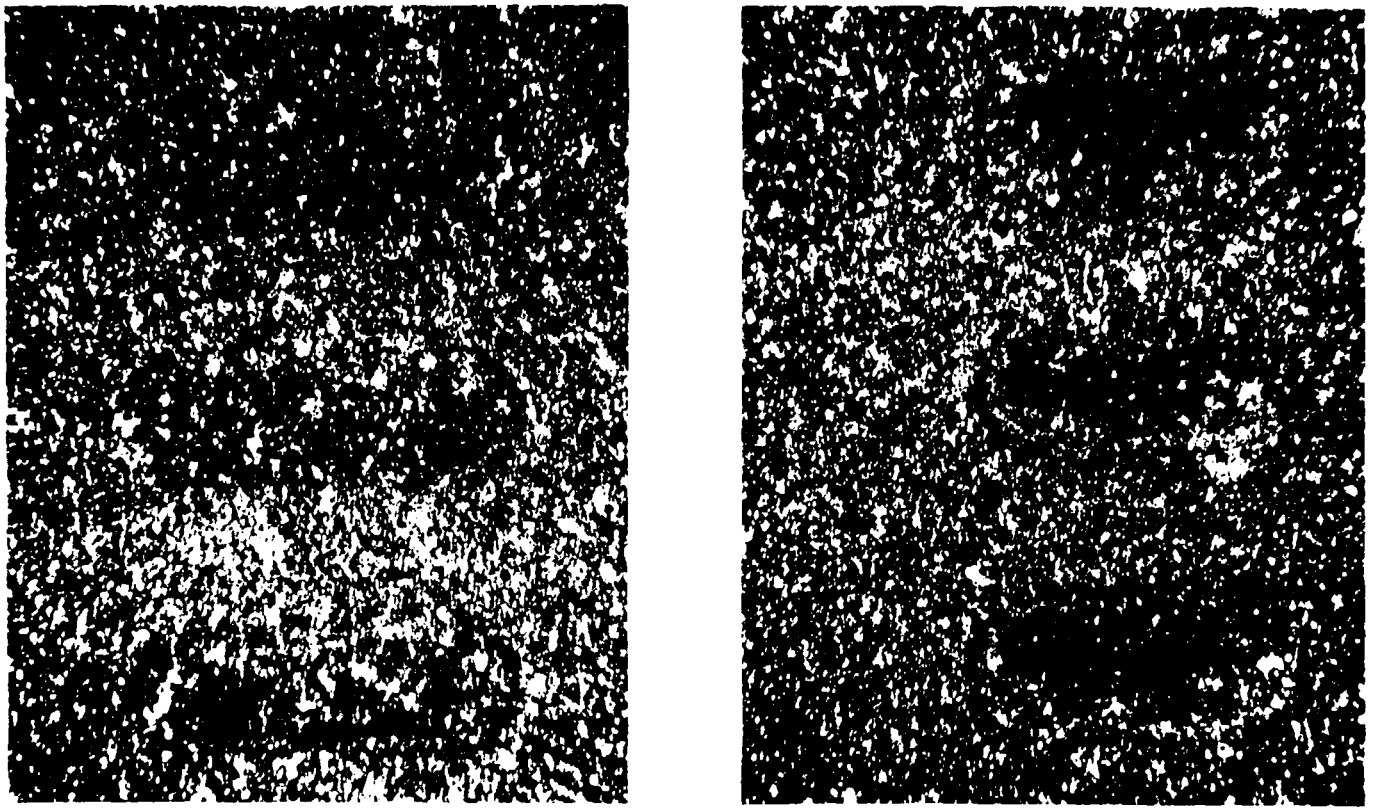

Fig. 3.5
OPTICAL MICROSCOPY VIEW OF GOLD DEPOSIT LINES PRODUCED VIA PULSE LASER IRRADIATION ON SUPERCONDUCTIVE CERAMIC SUBSTRATE. [SEE TABLE 3.2 , SAMPLE E , EXP. IX]
A. LASER IRRADIATION 30 PULSES/SITE B. LASER IRRADIATION 50 PULSES/SITE

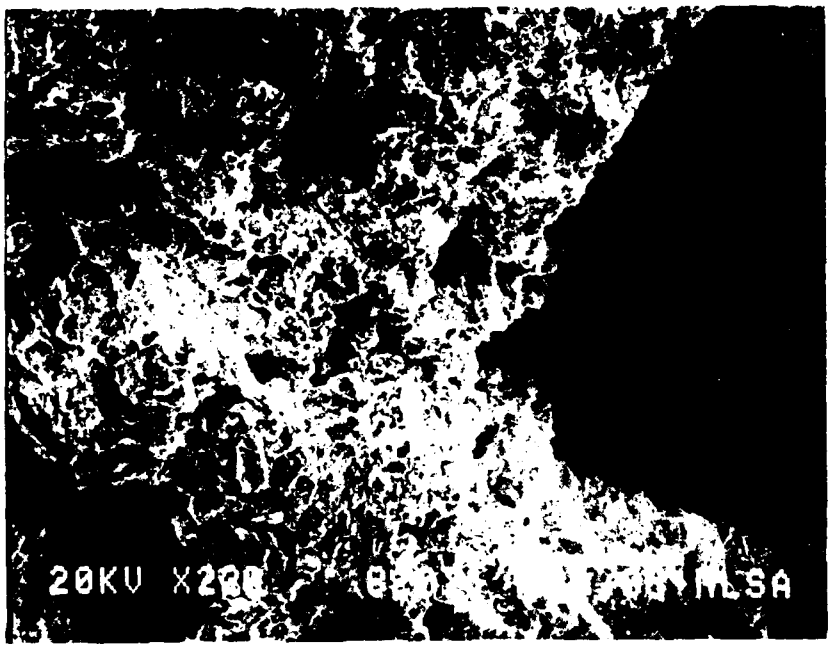

Fig. 3.6
TYPICAL SEM VIEW OF LASER IRRADIATED AREA INDICATING DAMAGE IN FORM OF HOLES (DARK AREA) IN THE SUPERCONDUCTIVE CERAMIC SUBSTRATE AS WELL AS FORMATION OF GOLD DEPOSIT AROUND THE HOLE. [SEE TABLE 3.1 , SAMPLE A , EXP. I , LINE 4]
No. OF LASER PULSES PER SITE WERE 1000 AT ENERGY LEVEL ABOVE 2mj/PULSE

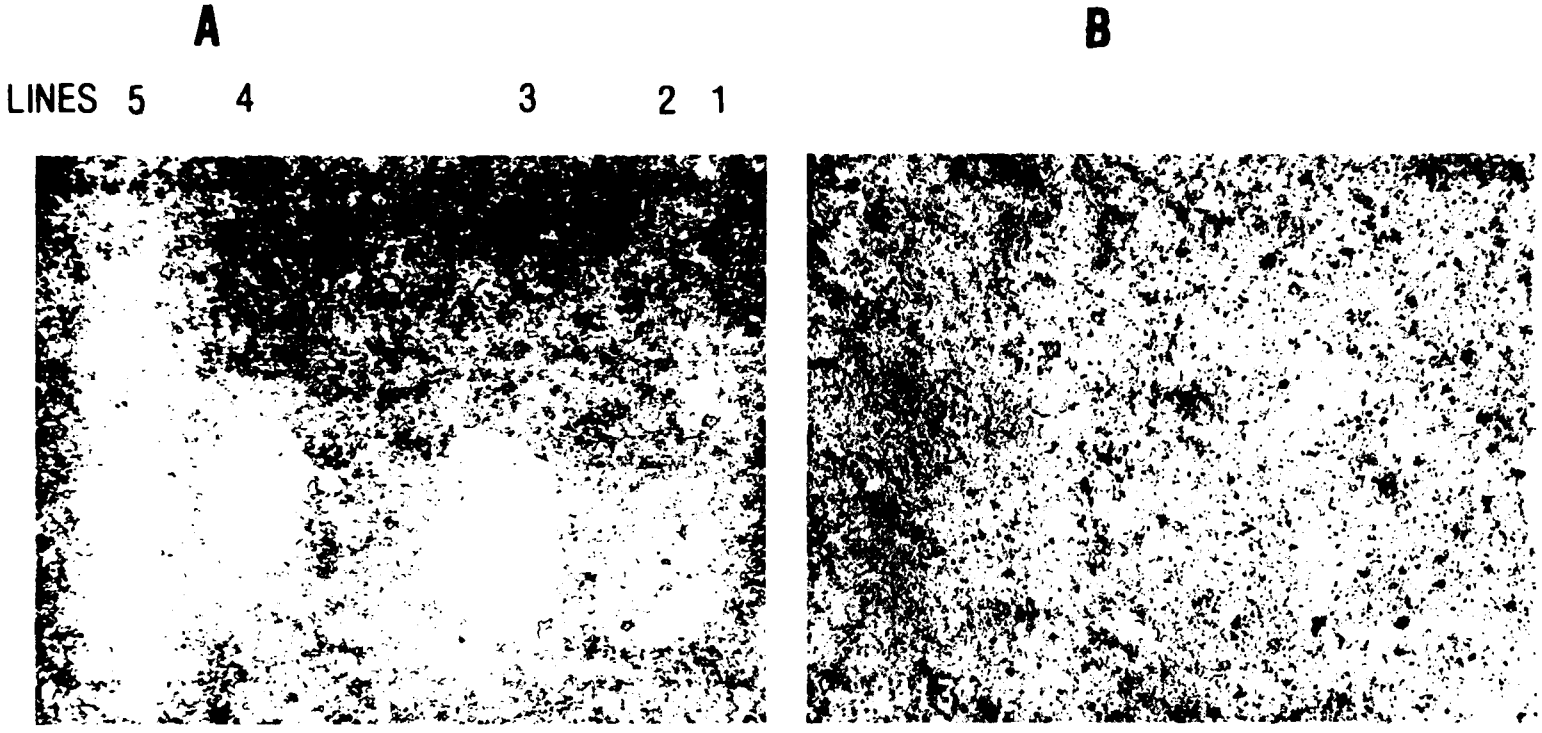

Fig. 3.7
TYPICAL SEM VIEW OF GOLD DEPOSIT LINES FORMED ON SUPERCONDUCTIVE CERAMIC SPECIMEN VIA PULSE LASER IRRADIATION. [SEE TABLE 3.1 , SAMPLE A , EXP. III , LINES 1-5] A. BACKSCATTERED ELECTRON IMAGE OF GOLD LINES. B. SECONDARY ELECTRON IMAGE OF GOLD LINES. LINES ARE NOT DETECTED IN THAT IMAGE

any surface damage at the gold deposit areas or outside these areas (Figure 3.7.B). Furthermore the gold lines (Figure 3.7.A) appeared to be continuous following the topography and the pores in the superconductive ceramic substrates. Typical analyses of the gold deposit lines are shown in Figure 3.8. The presence of gold as well as of copper, yttrium, barium, and chloride was detected. It might be noted that the chloride came from the plating solution which contained $HAuCl_4$ gold compounds. However, the percentage of the chloride in the deposit was only about 3.48% wt compared to 20% wt of gold. The elements of Cu, Ba and Y are in the superconductive ceramic material Y-Ba-Cu-O base compound.

Typical surface morphology of gold deposit pads is shown by SEM in secondary and backscattered electron images (Figure 3.9, 3.10, 3.11). The pads were formed on superconductor ceramic material as shown optically in Figure 3.4. In Figure 3.9 the nonirradiated area can be seen. At low magnification (Figure 3.9.A.) the surface appeared to have a cell type structure consisted also with many pores.

High magnification pictures (Figures 3.9.B., 3.9.C.) of the surface indicated the presence of grains about 10 μm in size as well as cracks and microcracks (Figure 3.9.C). Secondary electron images of the gold pad surface (Figure 3.10) indicate the presence of holes and pores, as well as microcracks. However the gold deposit followed these topographies. No substrate damage due to the laser irradiation was observed especially when one compares the nonirradiated surface (Figure 3.9) with the irradiated area (Figure 3.10).

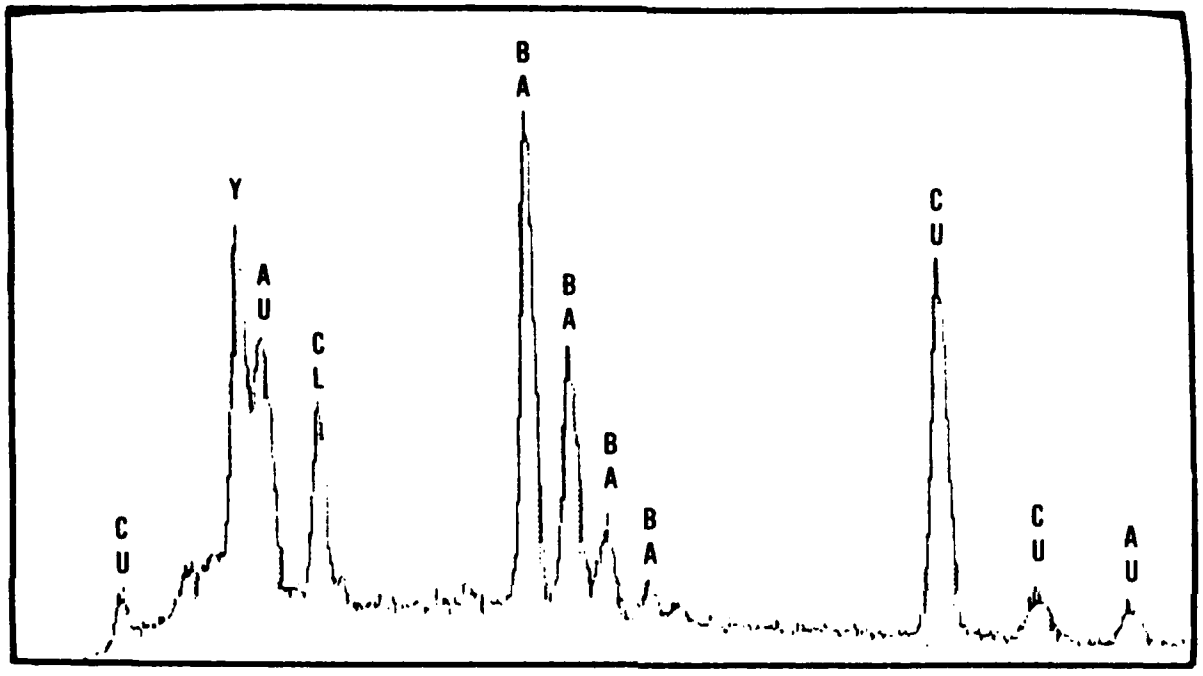

NO. OF ITERATIONS 3

-----	K	[Z]	[A]	[F]	[ZAF]	ATOM.%	WT.%	
Y -L	0.137	0.971	1.473	0.992	1.419	17.73	16.66	*
AU-M	0.161	1.109	1.318	1.000	1.461	9.64	20.05	
CL-K	0.029	0.848	1.654	0.996	1.396	9.42	3.48	*
BA-L	0.331	1.066	1.071	0.994	1.134	22.18	32.08	
CU-K	0.342	0.918	1.052	0.984	0.950	41.03	27.72	

* - HIGH ABSORBANCE

FIG 3.8: TYPICAL EDX ANALYSIS PROFILE OF GOLD DEPOSIT LINES SHOWN IN FIGURE 3.7. THE PRESENCE OF GOLD AS WELL AS OF Y, Ba, Cu IS SHOWN CLEARLY. ALSO RESIDUES OF Cl ARE DETECTED IN THE RANGE OF 3.48 WT% COMPARED TO 20.05 WT% OF GOLD.

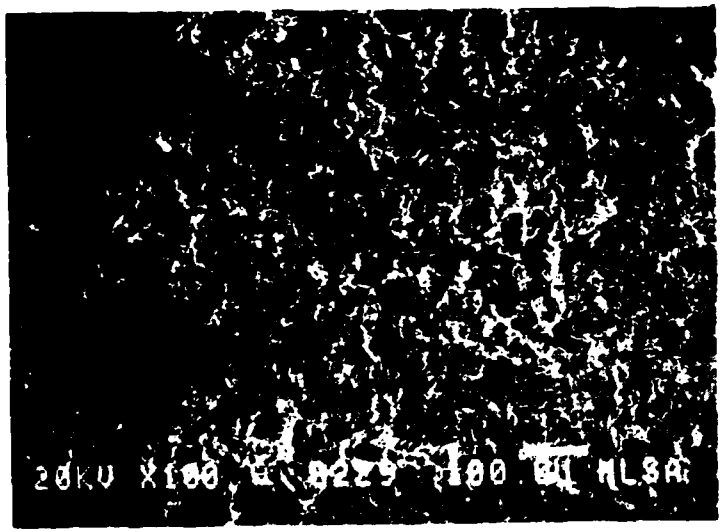

A

B

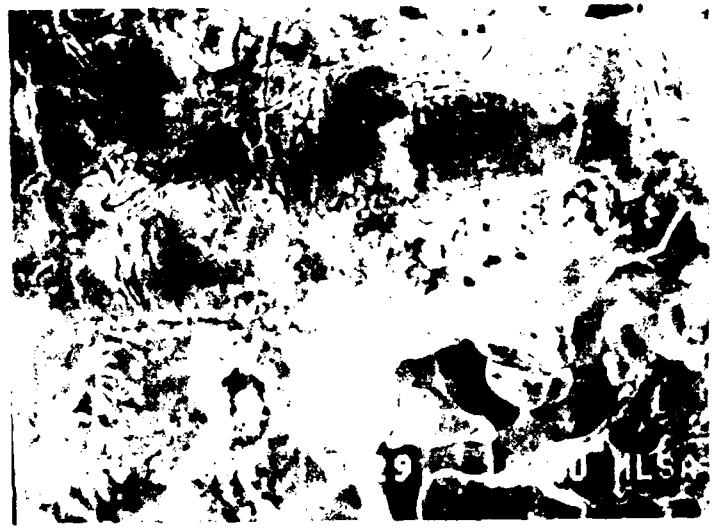

Fig. 3.9
TYPICAL SEM SECONDARY IMAGE VIEW OF SUPERCONDUCTIVE CERAMIC SPECIMEN AT NON IRRADIATED AREA. [SEE TABLE 3.2, SAMPLE C]
A. GERERAL LOW MAG VIEW
B. ENLARGEMENT OF THE AREA SHOWN IN (A) C. HIGH MAG VIEW OF THE AREA SHOWN IN (B)

C

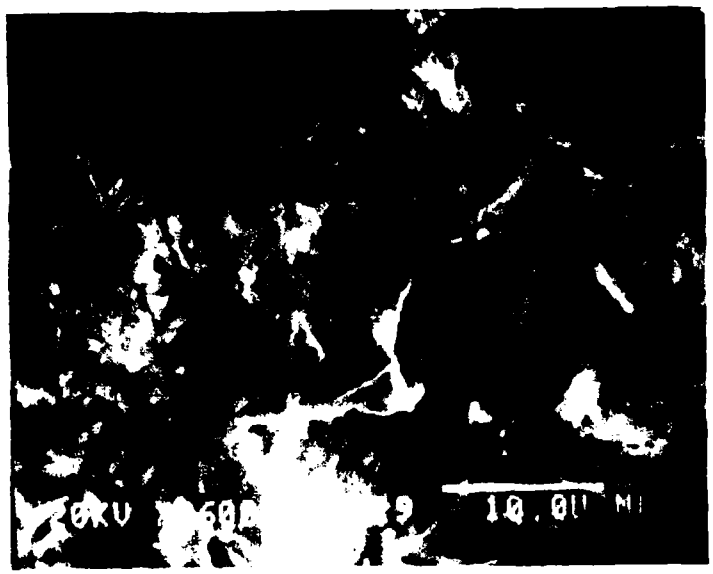

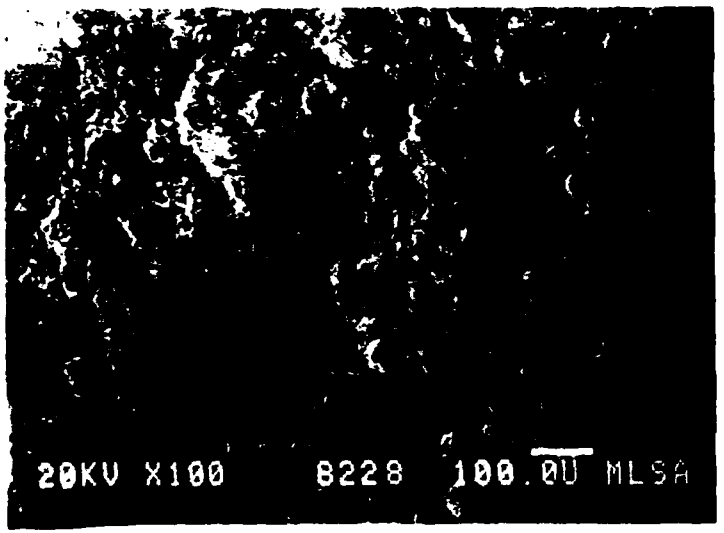

A

B

Fig. 3.10
TYPICAL SEM SECONDARY ELECTRON IMAGES OF GOLD DEPOSIT ZONES VIA PULSE LASER IRRADIATION OF 20 PULSES/ SITE. [SEE TABLE 3.2, SAMPLE C, ZONE 2] A. LOW MAG OVERALL VIEW B. HIGHER MAG OF THE AREA SHOWN IN (A) C. HIGH MAG OF THE AREA SHOWN IN (B)

C

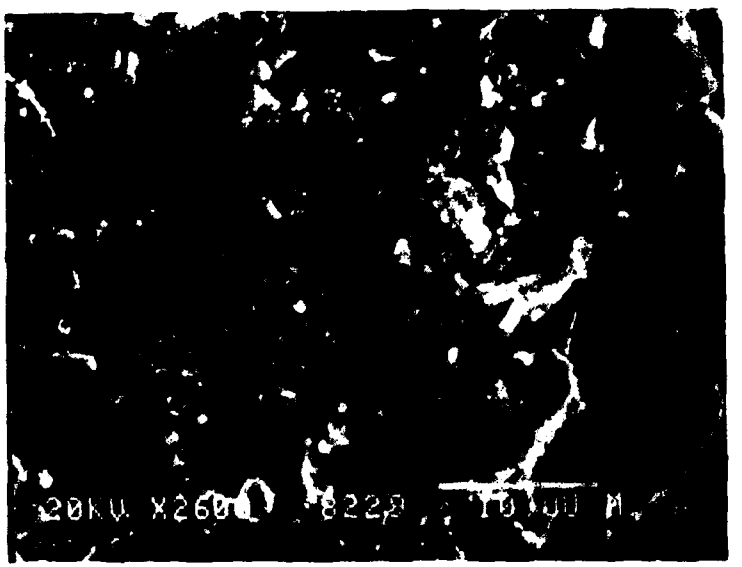

Typical SEM Backscattering electron images of gold pads on superconductive ceramic substrates are shown in Figure 3.11. The bright zone in Figure 3.11.A indicates the presence of gold deposits. The boundary between the gold deposit and the nonirradiated area (dark zone in Figure 3.11.A) is shown very clearly. The Backscattered electron image of the gold pad surface is shown in Figure 3.11.B and its topographic view is shown in Figure 3.11.C. Gold deposits covered all the hills and valleys on the superconductor ceramic surface. Furthermore, formation of the gold pad via pulse laser irradiation did not introduce damage or any other changes in the substrate surface.

Figure 3-12 shows typical gold pads produced via pulse laser irradiation at 30 pulses/site (Figure 3.12.A) and at 50 pulses/site (Figure 3.12.B). These pictures might indicate the effect of the number of pulses on the amount and growth of the gold deposit. The higher the number of pulses, the thicker or denser was the gold deposit. The boundary between the gold deposit and the bare surface is shown in Figure 3.13.A (bright zone indicated the presence of gold). Enlargement of the gold covered zone in Figure 3.13.A revealed the presence of grain structure in the ceramic surface (Figure 3.13.B). Gold deposits covered these grains which were 10 to 20 μm in size.

3.2.3 AES and ESCA Observations

Typical AES and ESCA profile analyses of gold deposit pads shown in Figure 3.3 (See Table 3.2, Sample B, Exp. VII) are shown in Figures 3.14, 3.15 and 3.16 respectively.

Figure 3.14 shows an AES surface analyses profile of Sample B at nonirradiated laser area which was away from the two gold pads shown

A

B

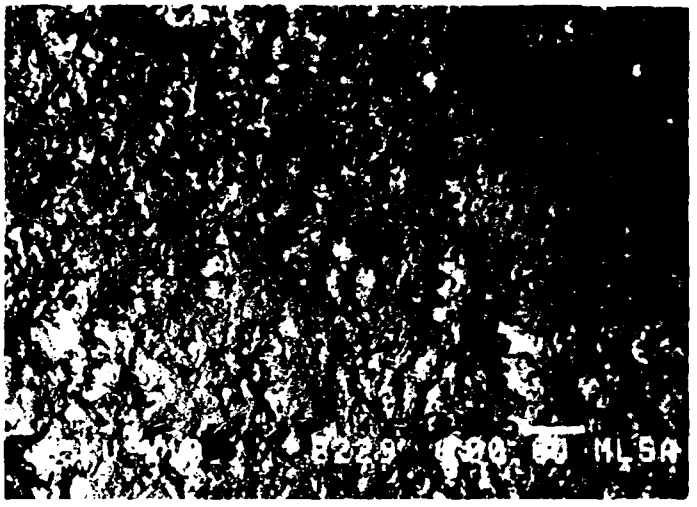

Fig. 3.11
TYPICAL SEM BACKSCATTERED ELECTRON IMAGES (TILTING 25°) OF GOLD DEPOSIT ZONES VIA PULSE LASER IRRADIATION AT 20 PULSES/SITE. [SEE TABLE 3.2, SAMPLE C, EXP VI, ZONE 2]
A. BRIGHT ZONE INDICATING THE PRESENCE OF GOLD ON IRRADIATED AREA. DARK ZONE INDICATING NON IRRADIATED AREA AND NO GOLD PRESENCE.
B. HIGHER MAG OF THE GOLD DEPOSIT (BRIGHT AREA) SHOWN IN (A) C. TOPOGRAPHY BACKSCATTERED IMAGE OF THE GOLD AREA SHOWN IN (B)

C

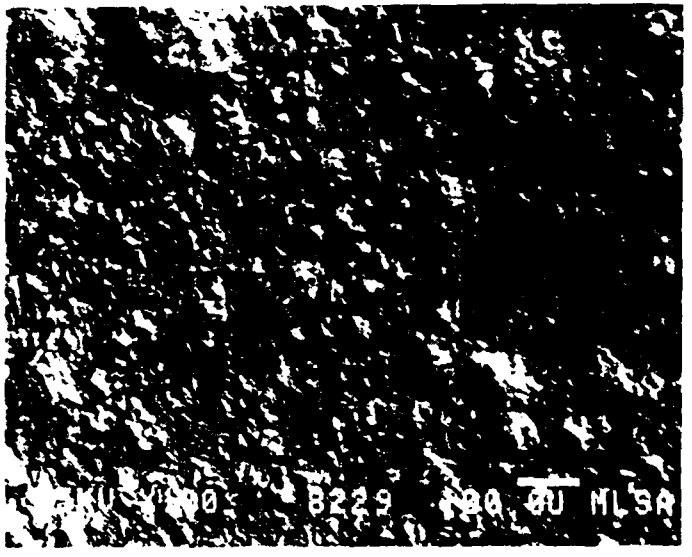

A

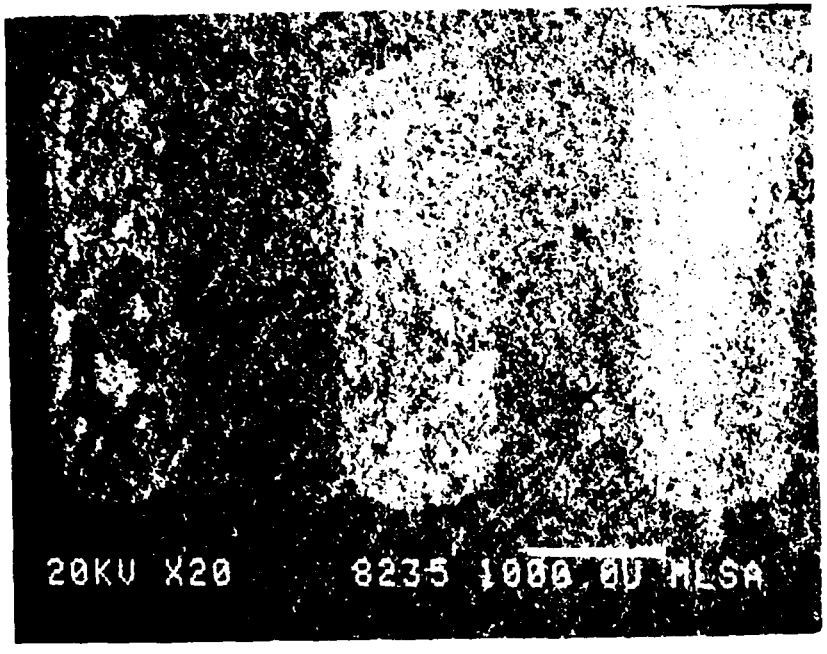

B

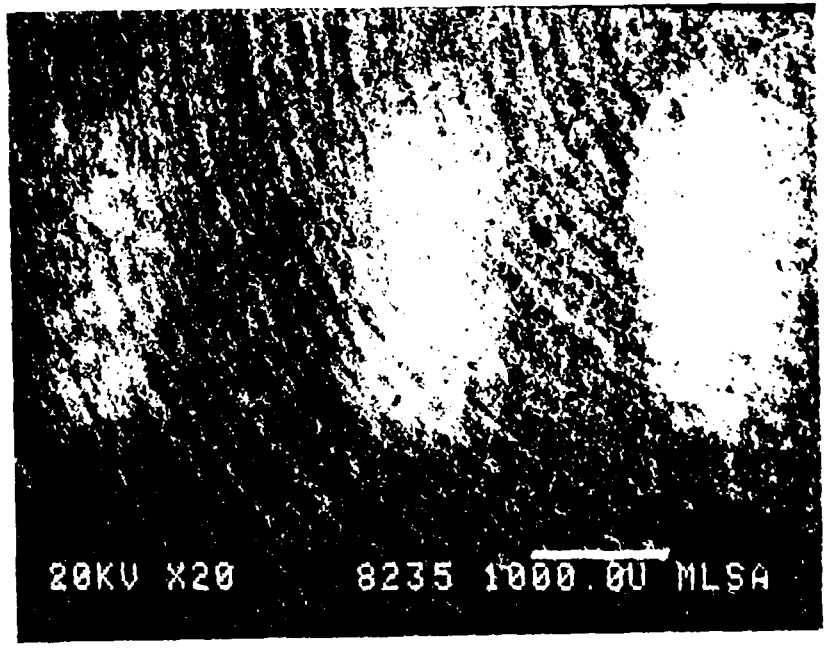

Fig. 3.12

SEM SECONDARY ELECTRON IMAGE OF GOLD DEPOSITE LINES PRODUCED VIA PULSE LASER IRRADIATION ON SUPERCONDUCTIVE CERAMIC SUBSTRATE. [SEE TABLE 3.2 , SAMPLE E , EXP IX] A. LASER IRRADIATION 30 PULSES/SITE B. LASER IRRADIATION 50 PULSES/SITE

A

B

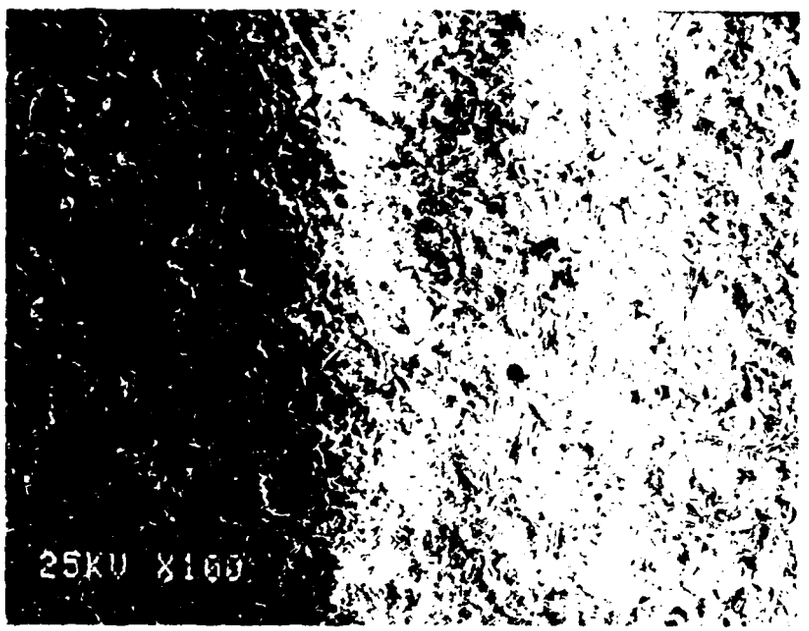

Exp. 3.13
SEM SECONDARY ELECTRON IMAGE OF GOLD DEPOSIT PRODUCED VIA PULSE LASER IRRADIATION ON SUPERCONDUCTIVE CERAMIC SUBSTRATE. [SEE TABLE 3.2 , SAMPLE E , EXP. IX]
A. LASER IRRADIATION 50 PULSES/SITE. BRIGHT ZONE IS GOLD DEPOSIT ZONE. DARK ZONE IS NON IRRADIATED AREA.
B. ENLARGEMENT OF DEPOSIT GOLD AREA SHOWN IN (A)

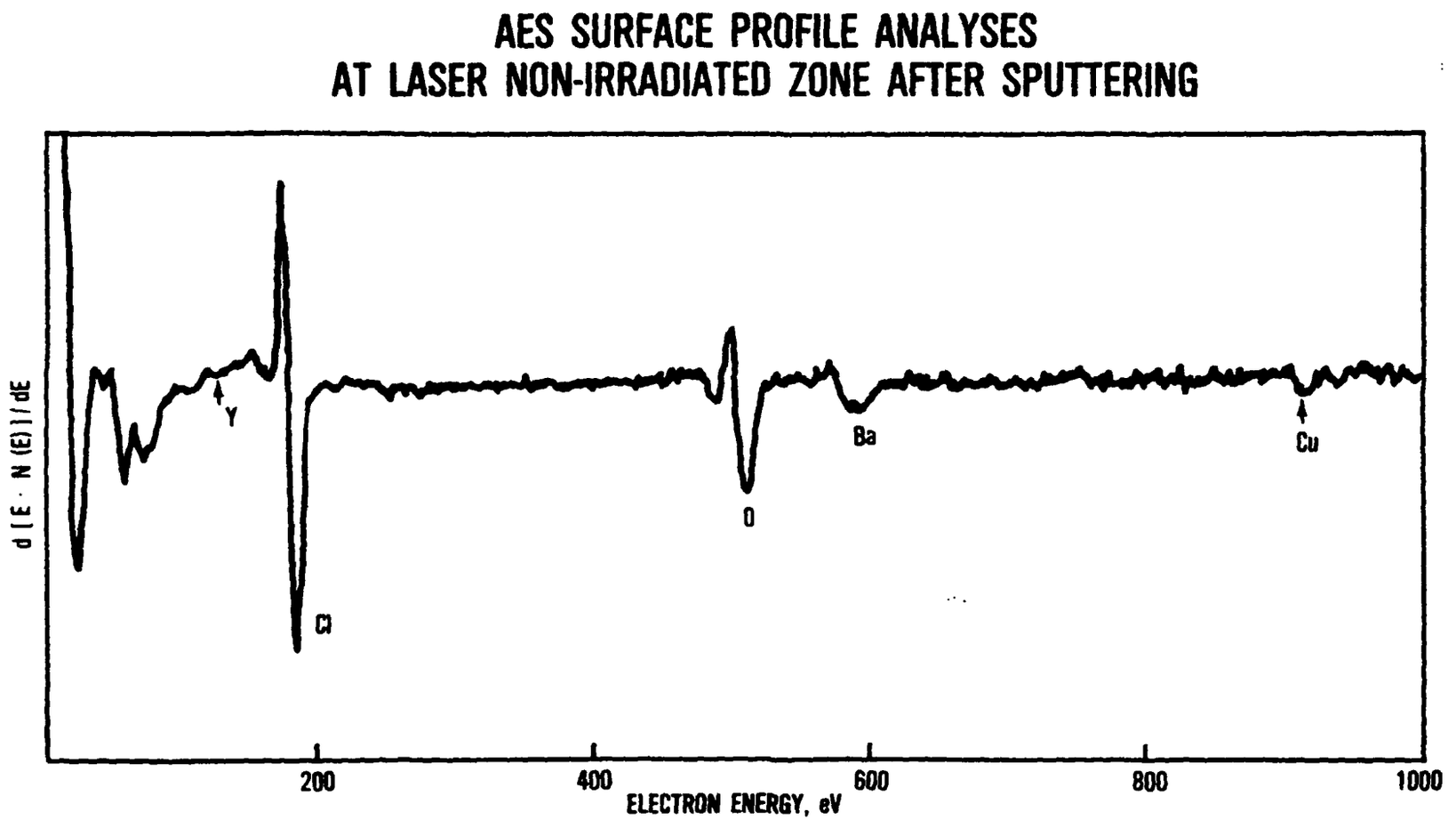

FIG 3.14: AES SURFACE ANALYSES PROFILE AT LASER NON-IRRADIATED ZONE. SURFACE WAS EXAMINED AFTER SPUTTERING WITH Ar ions. [TABLE 3.2, EXP VII, SAMPLE B].

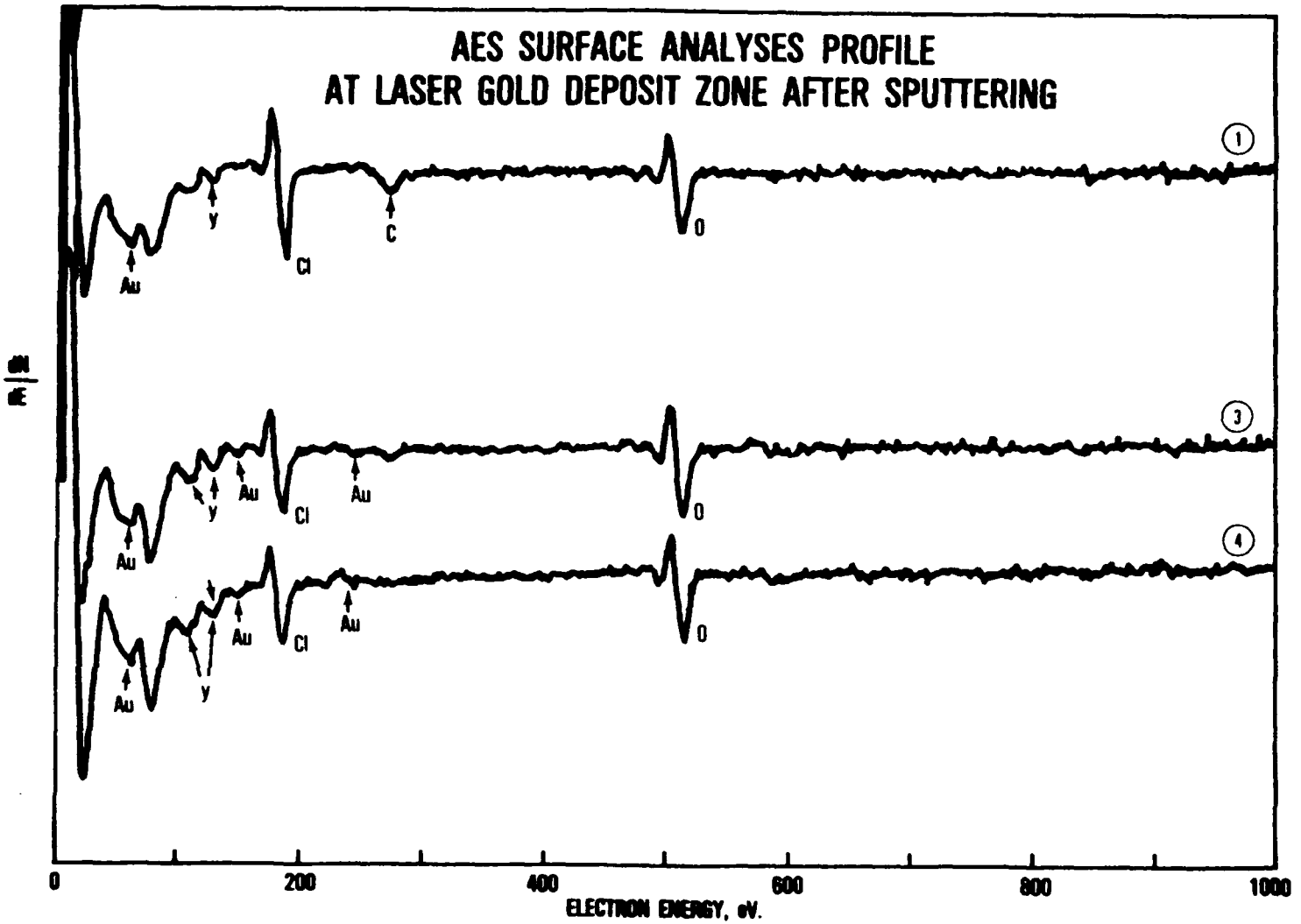

FIG. 3.15: AES SURFACE ANALYSES PROFILE AT LASER GOLD DEPOSIT ZONE AFTER VARIOUS TIMES OF ION SPUTTERING [SEE TABLE 3.2, SAMPLE B, EXP VII ZONE 1) LASER IRRADIATION WAS KEPT AT 30 PULSES / SITES. AES PROFILES NO 1, 3, 4 WERE TAKEN AFTER VARIOUS TIME OF SPUTTERING BASICALLY THE PROFILES INDICATE THE PRESENCE GOLD, CHLORINE AND OXYGEN

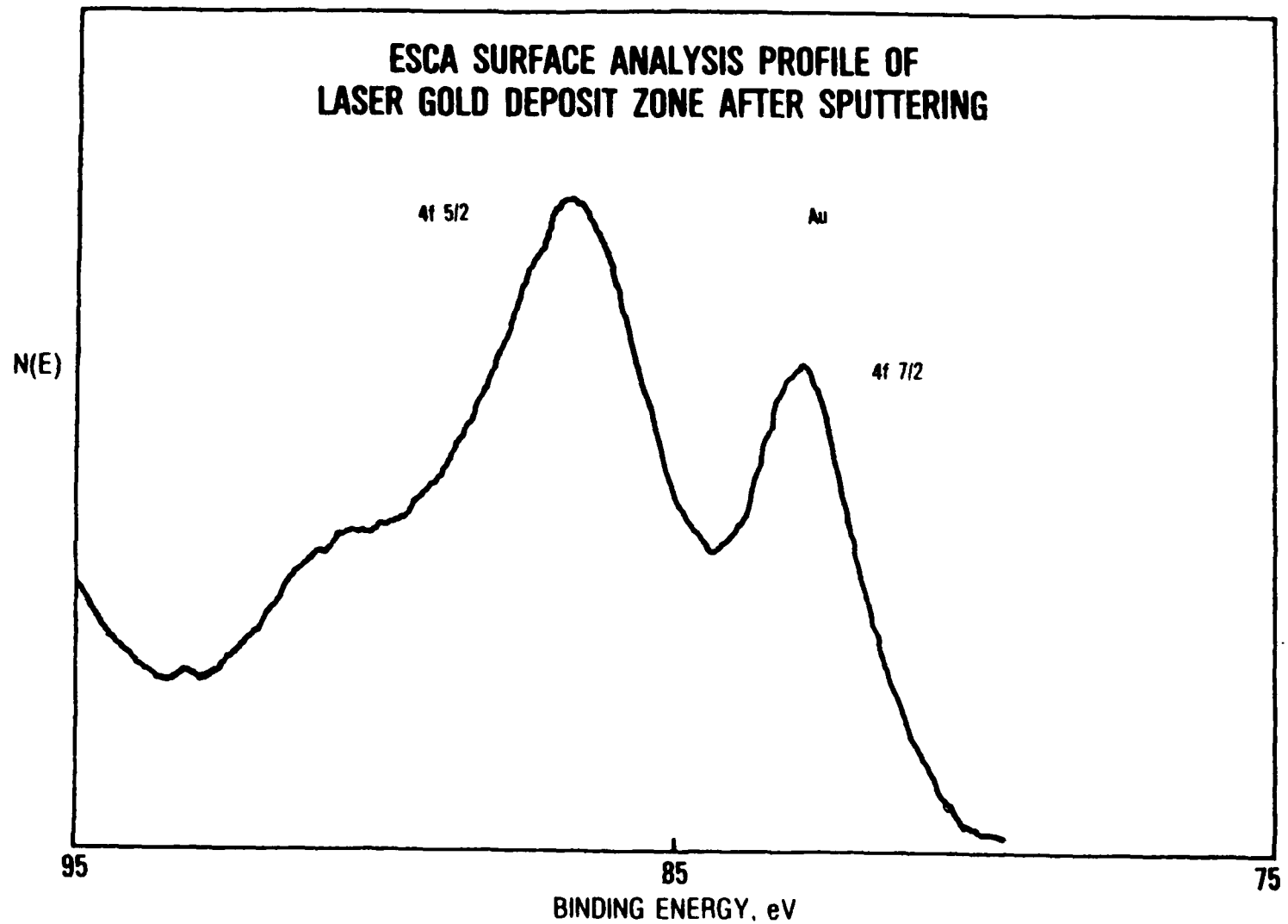

FIG 3.16: ESCA SURFACE ANALYSIS PROFILE OF LASER GOLD DEPOSIT ZONE AFTER SUPUTTERING. [SEE TABLE 3.2, SAMPLE B, EXP VII, ZONE 2]. LASER IRRADIATION WAS KEPT AT 30 PULSES / SITE. THE PEAKS SHOWN INDICATE THE PRESENCE OF PURE ELEMENTAL GOLD WITH SOME GOLD COMPOUND

in Figure 3.3.A. The profile which was taken after ion sputtering shown the presence of Cu, Bu, O, Y which composed the superconductor Y-Bu-Cu-O base ceramic material. In addition the presence of Cl is very obvious. The Cl residue came from plating gold solution.

AES profile analyses of the gold deposit pad which was shown in Figure 3.3.A, Pad No. 2 is given in Figure 3.15. Three profiles are shown in Figure 3.15. They were taken after various times of ion sputtering of the gold deposit surface. It might be seen from profile No. 1,3,4 the presence of oxygen, chloride, gold and yttrium. No carbon, copper and barium was detected at the gold deposit pad. That is to say that the gold coverage thickness of the ceramic substrate surface was a good one. Furthermore, non-gold compounds were observed as can been seen in an ESCA profile analysis of the same gold pad (Figure 3.3.A, Pad No. 2). The ESCA surface analyses profile is shown in Figure 3.16 where the gold 1 7/2 and 1 5/2 peaks are clearly shown indicating the presence of pure elemental gold.

Further examinations of gold deposit pad composition and in particular the presence of pure elemental gold were conducted on Sample F, Exp X, Zone 2 where laser irradiation per site was 5 pulses (See Table 3.2, Sample F, Exp. X). A typical AES surface profile of that gold pad without sputtering is shown in Figure 3.16.A. The presence of Au is shown together with Cl, C, O, Ba, and Cu. The presence of Y-Ba-Cu-O was not surprising since these are the elements in the ceramic substrate. However their presence at the gold deposit surface indicated that either the gold deposit did not cover the whole area to 100% coverage due to surface roughness, or that the

gold deposit under these conditions was not completely continuous. An ESCA surface profile analyses of the same gold deposit pad surface (Table 3.2, Sample F, Exp. X, Zone 2) without sputtering are shown in Figure 3.16.B and Figure 3.16.C. The presence of pure elemental gold in the gold deposit pad is shown clearly from the gold peaks of Au (4d) and Au (4l) (Figure 3.16.B). Enlargement of the Au (4f) peak is shown in Figure 3.16.C. Clearly the peaks of Au (4l 5/2) and Au (4l 7/2) are found to indicate that the gold in the gold deposit pad was really an elemental gold. That finding was important from the mechanism point of view of gold deposition via laser irradiation, as well as from the technical point of view. Namely use these gold deposit pads as ohmic contacts or conductive lines on the superconductive Y-Ba-Cu-O ceramic base material.

3.3 Bulk and Gold Deposit Electrical and Contact Resistance

3.3.1 Resistance Measurement at Ambient Temperature

Electrical measurements for evaluating electrical resistance of gold deposits on superconductive Y-Ba-Cu-O base ceramic material were conducted making use of two probe points and four probe points.

The results obtained with two probe points are given in Figures 3.17, 3.18, 3.19 and in Tables 3.3, 3.4, and 3.5 respectively. In Figure 3.17 typical I-V curves were obtained from measurement of electrical resistance of a superconductor ceramic specimen before and after being immersed in gold ethanol solution. Table 3.3 indicated that the resistance measured of bulk specimen before being immersed in plating solution was 20 ohms as compared to 33 ohms after being

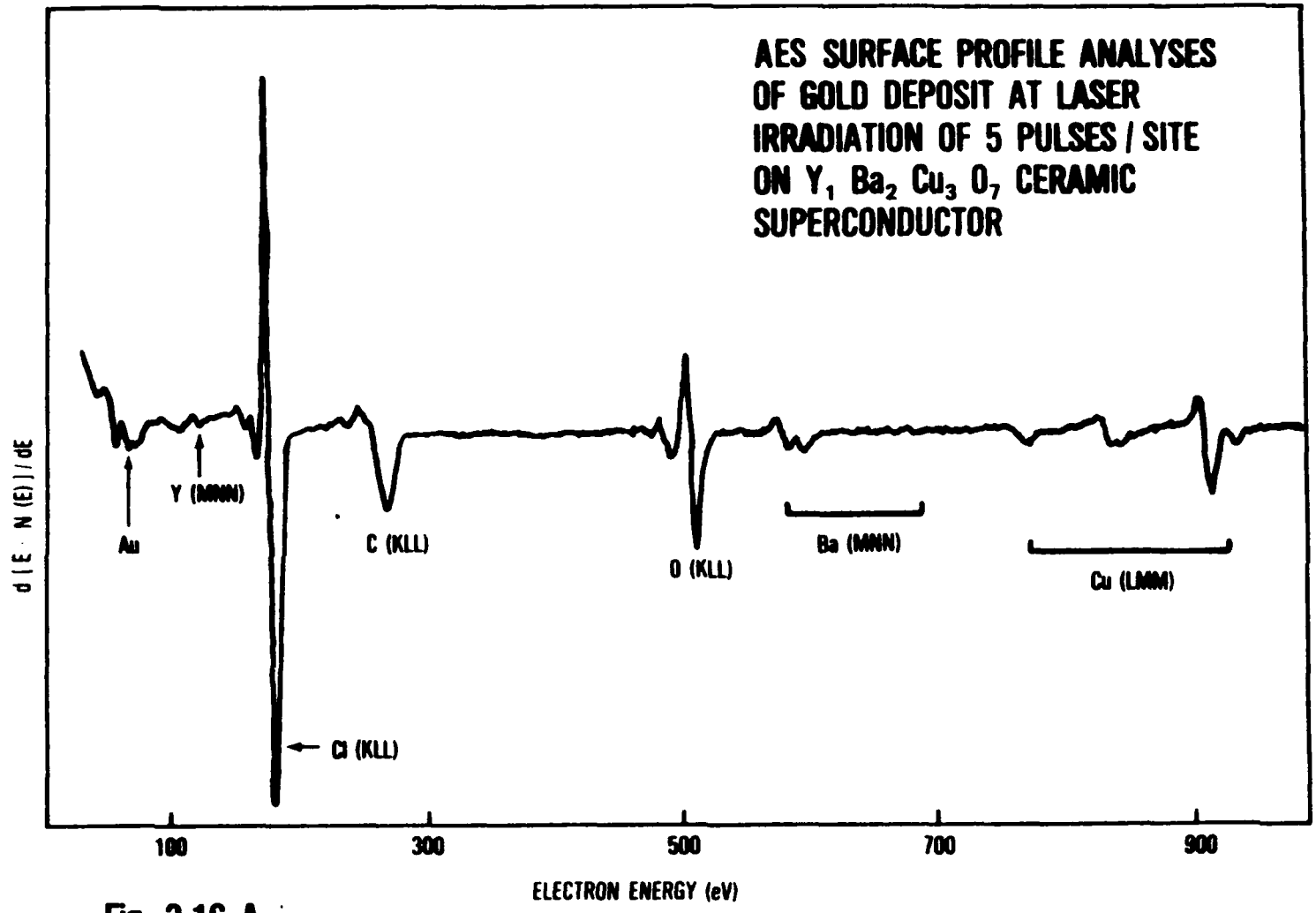

Fig. 3.16 A
AES SURFACE ANALYSES PROFILE OF GOLD DEPOSIT PAD FORMED VIA PULSE LASER IRRADIATION ON Y-Ba-Cu-O CERAMIC BASE MATERIAL [SEE TABLE 3.2, SAMPLE F, EXP X, ZONE 2]. THE ANALYSIS WAS CONDUCTED ON UNSPUTTERED SURFACE. THE PRESENCE OF GOLD, CHLORIDE, CARBON AS WELL AS OF YTTRIUM, BARIUM AND COPPER WERE DETECTED

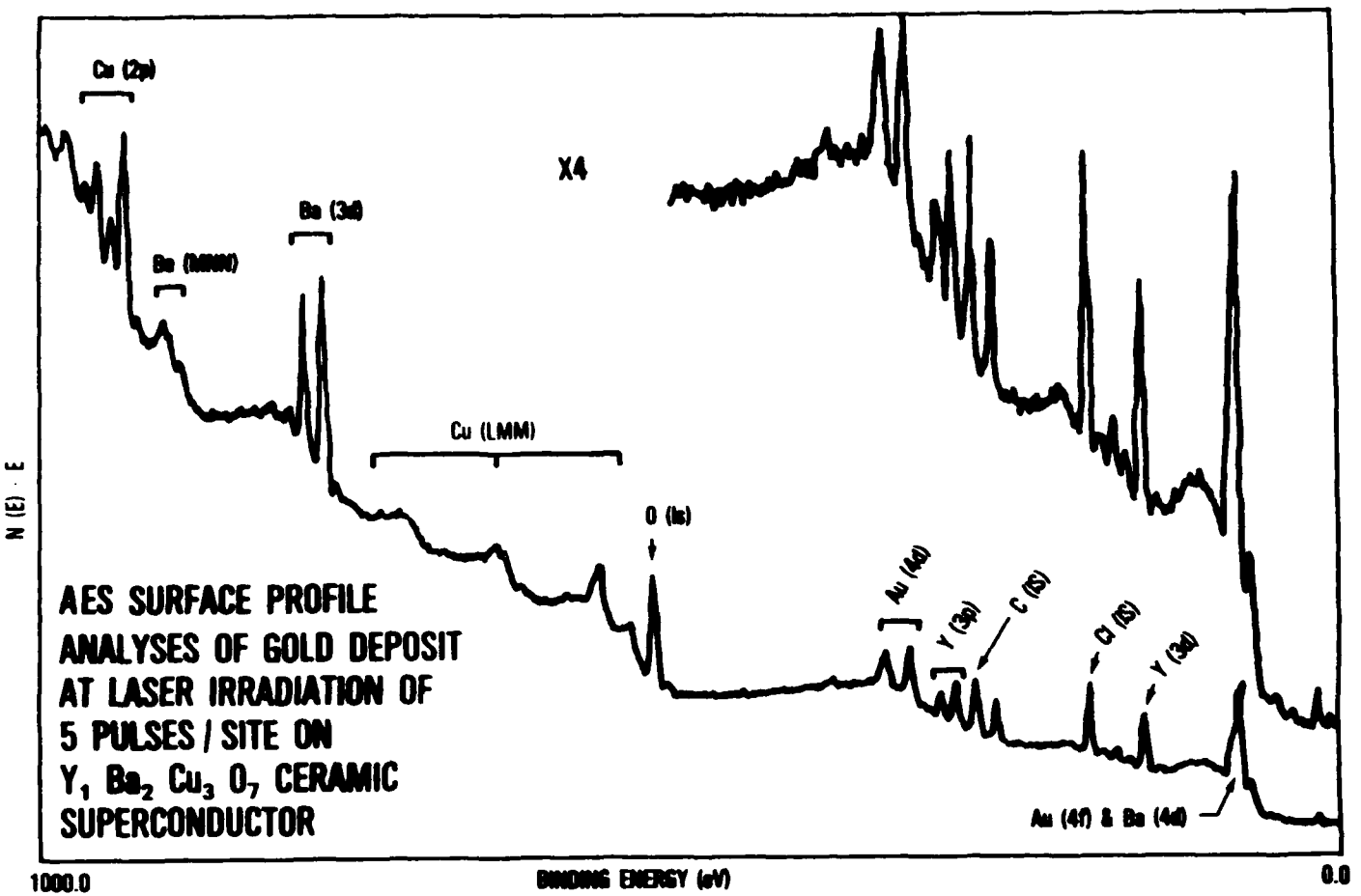

Fig. 3.16 B
ESCA SURFACE PROFILE ANALYSIS OF GOLD DEPOSIT PAD FORMED VIA PULSE LASER IRRADIATION ON Y-Ba-Cu-O CERAMIC BASE MATERIAL [SEE TABLE 3.2, SAMPLE F, EXP. X, ZONE 2]. THE ANALYSIS WAS CONDUCTED ON UNSPUTTERED SURFACE AND AT THE SAME LOCATION AS THE AES ANALYSIS (Fig. 3.16 A). THE PRESENCE OF PURE ELEMENTAL GOLD WAS FOUND BY DETECTING THE GOLD PEAKS OF Au(ud) AND Au(uf). ALSO THE PRESENCE OF COPPER BERIUM, YTTRIUM AS WELL AS CHLORINE, CARBON AND OXYGEN WERE THERE.

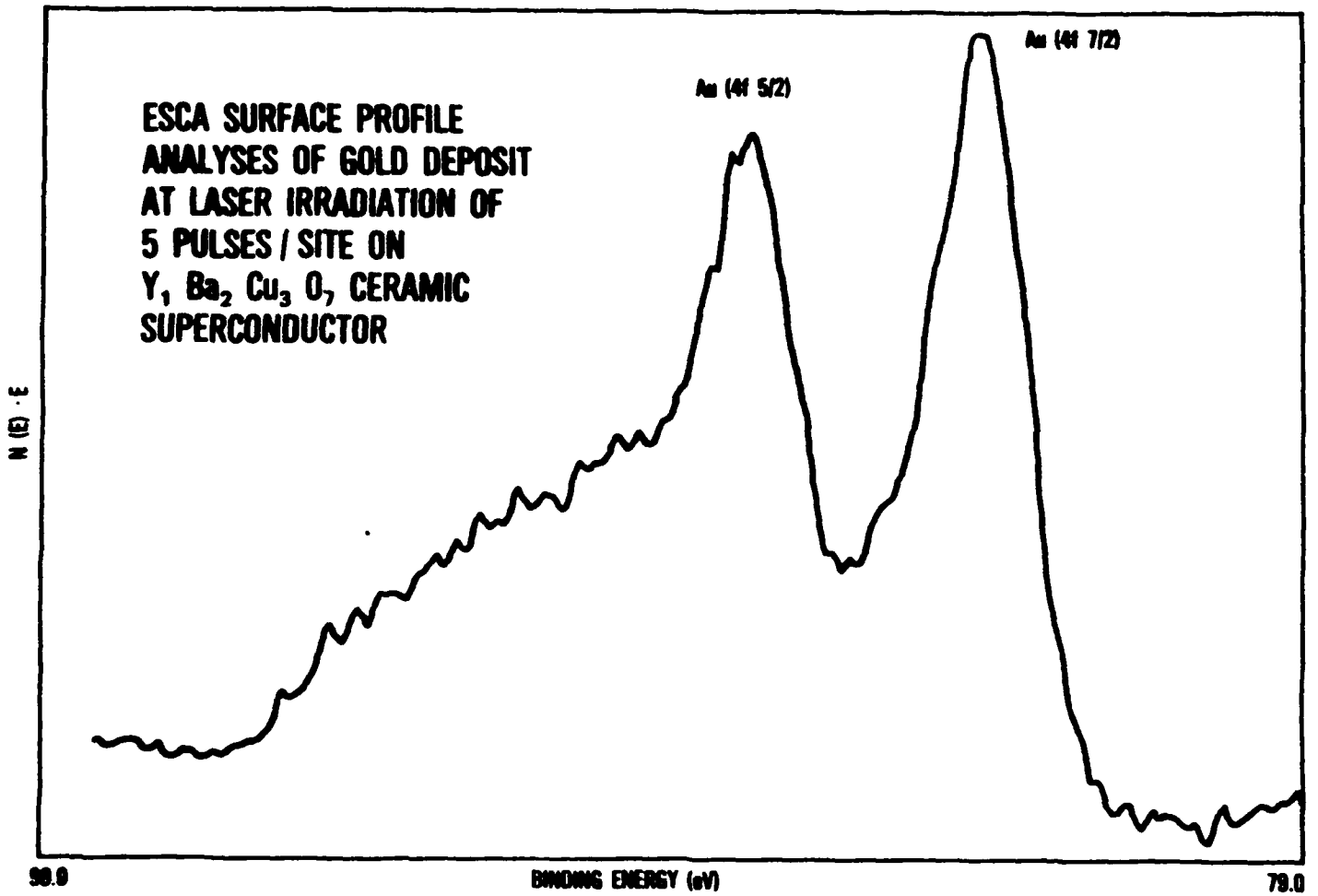

Fig. 3.16 C
ESCA SURFACE PROFILE ANALYSIS OF GOLD DEPOSIT PAD. THIS PROFILE IS EXPANSION OF THE ESCA PROFILE SHOWN IN Fig. 3.16 B. GOLD PEAKS OF Au(4f 5/2) AND Au(4f 7/2) ARE CLEARLY SHOWN INDICATING THE PRESENCE OF PURE ELEMENTAL GOLD IN THE GOLD DEPOSIT PAD
[SEE TABLE 3.2, SAMPLE F, EXP X, ZONE 2].

A

B

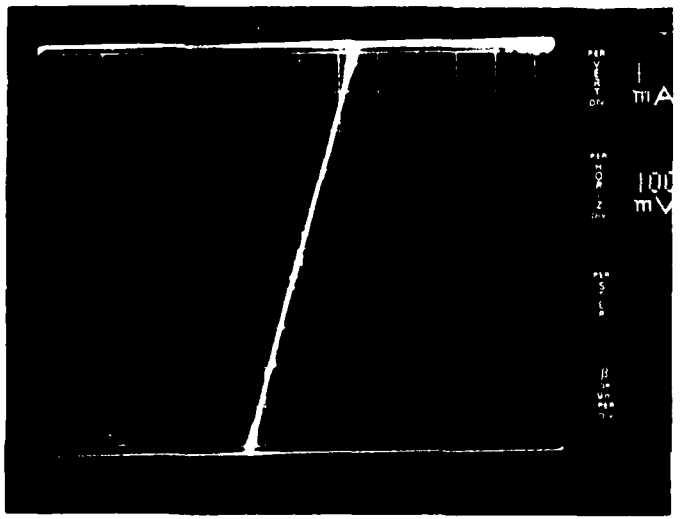

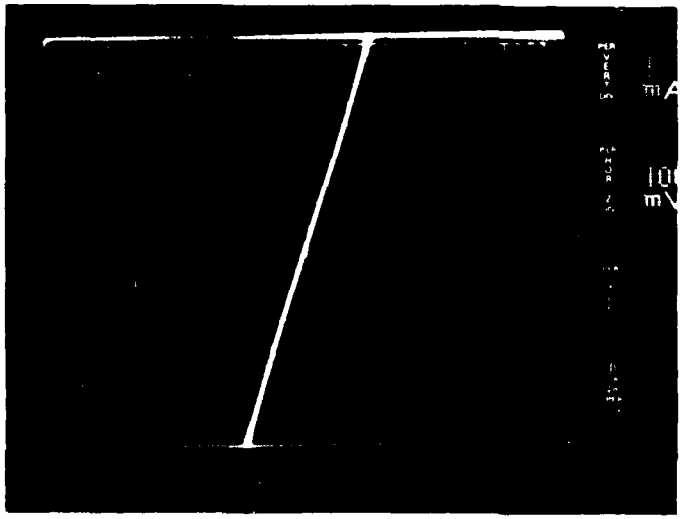

Fig. 3.17
TYPICAL I-V CURVES OBTAINED BY TWO PROBES ON SUPERCONDUCTIVE CERAMIC SUBSTRATE BEFORE AND AFTER BEING IMMERSED IN GOLD ETHANOL PLATING SOLUTION. [SEE TABLE 3.3]
A. BEFORE IMMERSION B. AFTER IMMERSION

TABLE 3.3

TWO POINT PROBES RESISTANCE OF

SUPERCONDUCTIVE SPECIMEN BULK MATERIAL BEFORE

AND AFTER BEING IMMERSED IN GOLD-ETHANOL PLATING SOLUTION

METHOD AND CONDITIONS: RESISTANCE MEASUREMENT. TWO POINT PROBES SEPERATED ONE CROWN GOLD PLATED PROBES WERE USED. PROBES WERE 1mm IN DIAMETER.

SAMPLE	SPECIMEN BULK MATERIAL AS RECEIVED WITHOUT IMMERSION IN GOLD PLATING SOLUTION	SPECIMEN BULK MATERIAL AFTER BEING IMMERSED IN GOLD-ETHANOL PLATING SOLUTION, WASHED IN ETHANOL, ULTRASONICALLY CLEANED IN ETHANOL AND DRIED
A	30Ω	33Ω

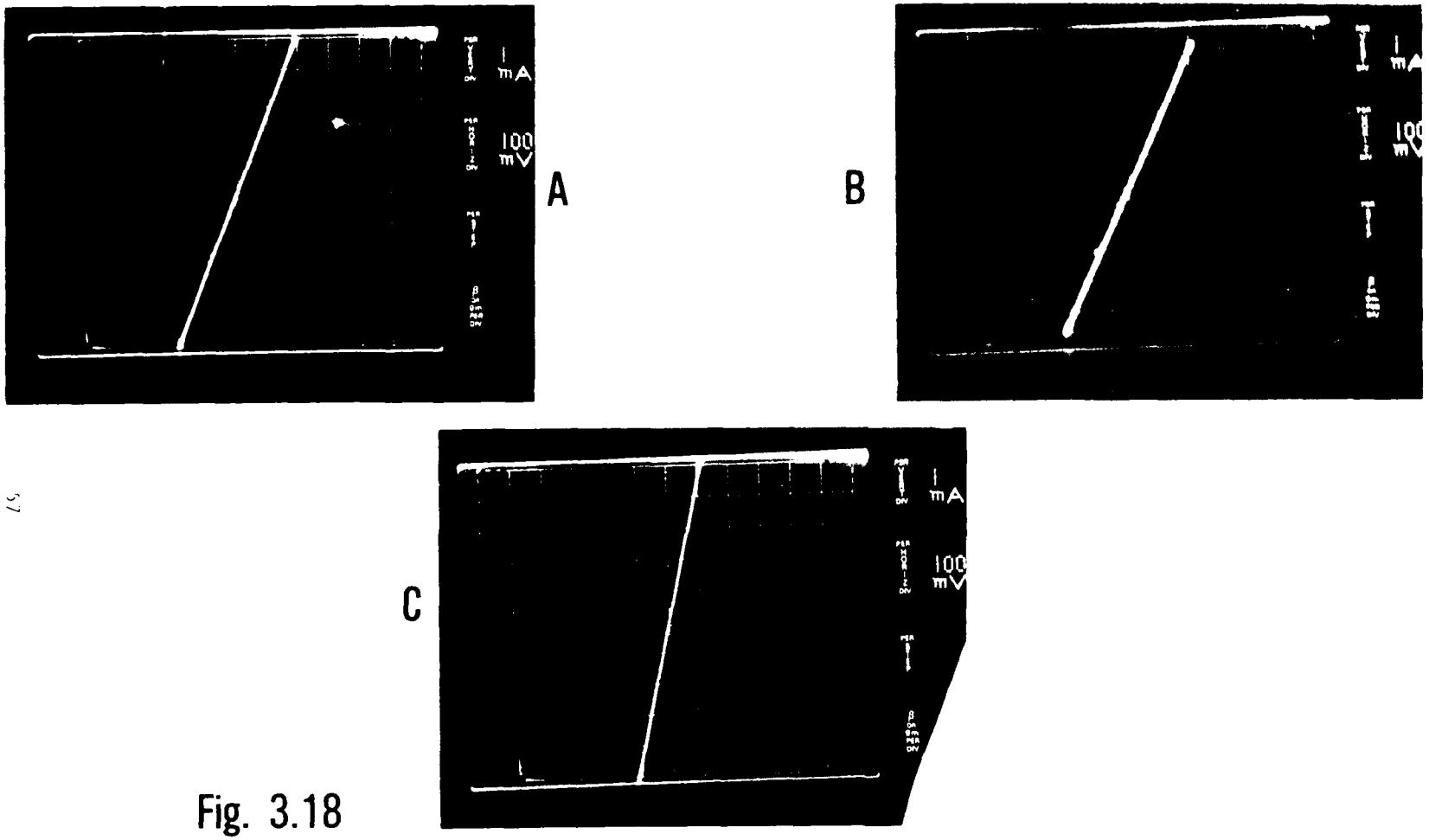

Fig. 3.18
TYPICAL I-V CURVES OBTAINED BY TWO POINT PROBES ON GOLD DEPOSIT LINES [SEE TABLE 3.1 , SAMPLE A , EXP. III , LINES 3, 4, 5] A. GOLD DEPOSIT LINE 3, 1000 PULSES/SITE
B. GOLD DEPOSIT LINE 4 100 PULSES/SITE
C. GOLD DEPOSIT LINE 5

TABLE 3.4

RESISTANCE MEASUREMENT OF TWO POINT PROBES LASER
GOLD LINE DEPOSITS ON SUPERCONDUCTIVE SPECIMEN MATERIAL MEASUREMENTS
WERE TAKEN AT AMBIENT TEMPERATURE

RESISTANCE MEASUREMENT OF GOLD DEPOST LINES BY TWO POINT PROBES. GOLD PLATED PROBES WERE USED WITH 1mm IN DIAMETER, WHILE MEASURING THE SPACING BETWEEN THE PROBES WERE 25mm.

SAMPLE NUMBER	EXPERIMENT NUMBER	GOLD LINE NUMBER	RESISTANCE OF GOLD LINE [Ω]	LASER NUMBER OF PULSES PER SITE	LASER BEAM MOVEMENT [μ]	LASER BEAM OVERLAP (%)	LASER BEAM ENERGY mj/pulse
A	III	3	35.70	1000	500	50	2.0
		4	45.45	100	500	50	2.0
		5	20.00	1	5	99.5	2.0

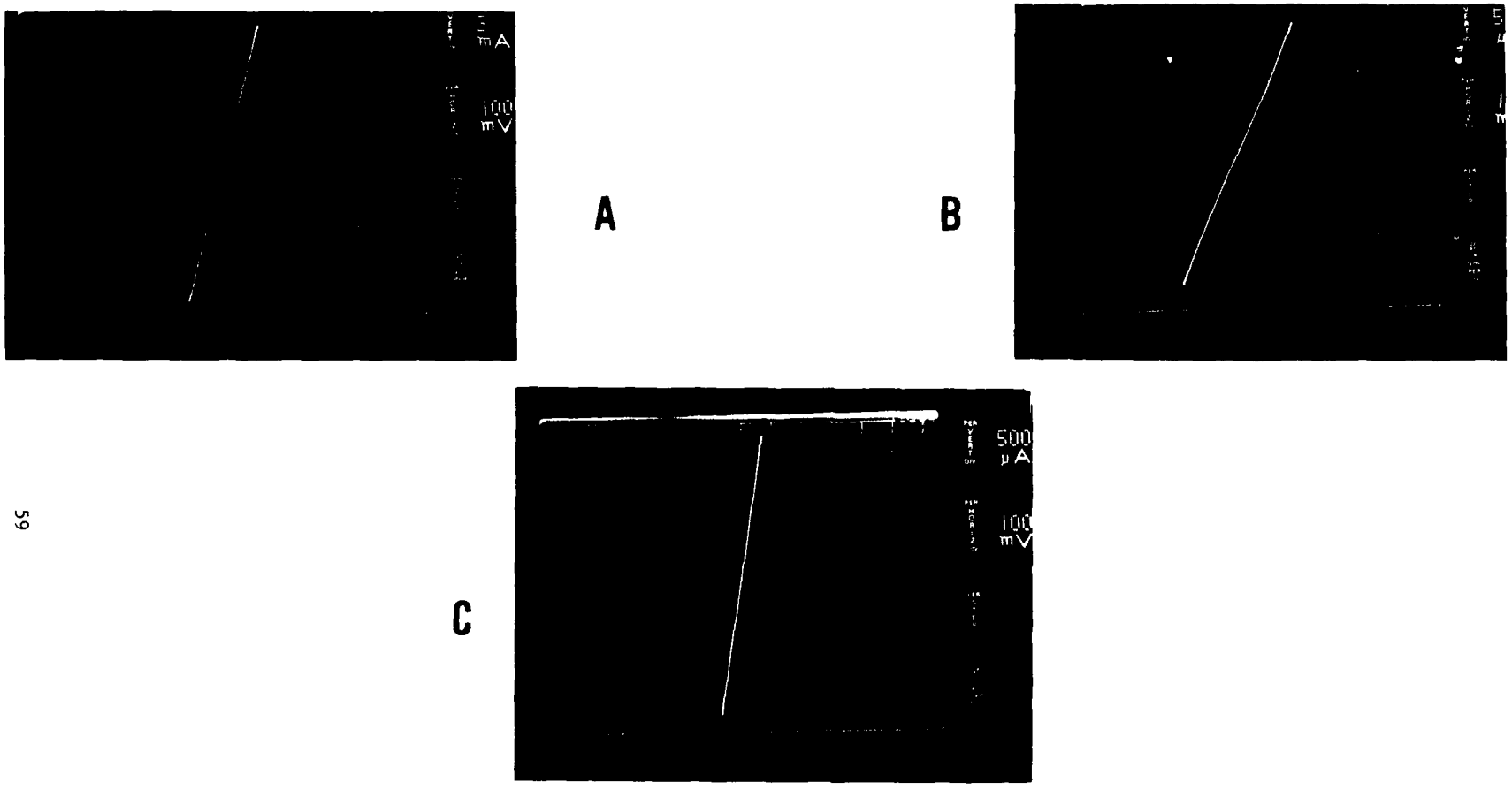

Fig. 3.19

TYPICAL I-V CURVES OBTAINED BY TWO POINT PROBES ON GOLD DEPOSIT LINES. [SEE TABLE 3.1 , SAMPLE B , EXP.V , LINES 3a, 4a] A. NON IRRADIATED AREA, NO GOLD DEPOSIT B. LASER IRRADIATION 100 PULSES/SITE, LINE 3a C. LASER IRRADIATION 200 PULSES/SITE, LINE 4a

TABLE 3.5

TWO POINT PROBES RESISTANCE MEASUREMENT OF SUPERCONDUCTIVE SPECIMEN MATERIAL AND OF LASER GOLD GOLD LINE DEPOSITS - MEASUREMENTS WERE TAKEN AT AMBIENT TEMPERATURE

RESISTANCE MEASUREMENT OF BULK SUPERCONDUCTIVE SPECIMEN MATERIAL AND OF GOLD DEPOSITS LINES BY TWO POINT PROBES. GOLD PLATED PROBES WERE USED WITH 1mm SPACING BETWEEN THE PROBES WHILE MEASURING. PROBES WERE 1mm IN DIAMETER.

SAMPLE NUMBER	EXPERIMENT NUMBER	GOLD LINE NUMBER	RESISTANCE OF GOLD LINE [Ω]	LASER NUMBER OF PULSES PER SITE	LASER BEAM MOVEMENT [μ]	LASER BEAM OVERLAP (%)	LASER BEAM ENERGY mj/pulse
B	---	---	12.5	---	---	---	---
	V	3A	66.0	100	50	95	2.0
		4A	30.0	200	50	95	2.0

TABLE 3.6

FOUR POINT PROBES RESISTANCE MEASUREMENTS OF SUPERCONDUCTIVE SPECIMEN MATERIAL AND CONTACT RESISTANCE MEASUREMENTS OF LASER GOLD DEPOSITS AT VARIOUS ZONES ON THE SUPERCONDUCTIVE SPECIMEN SURFACE - MEASUREMENTS WERE TAKEN AT AMBIENT TEMPERATURE

- FOUR POINT PROBES RESISTANCE MEAURING OF BULK SUPERCONDUCTIVE SPECIMEN MATERIAL WAS CONDUCTED WITH GOLD COATED PROBES HAVING 9 PINS OF 0.1mm IN DIAMETER AT THE PROBE CROSS SECTION AREA WHICH WAS 1MM IN DIAMETER. DISTANCE BETWEEN THE TWO MIDDLE PROBES MEASURING THE VOLTAGE DROP WAS 3mm. MEASUREMENTS WERE TAKEN AT CONSTANT CURRENT OF 100mA

- CONTACT RESISTANCES OF GOLD PAD DEPOSITS WERE MEASURED WITH TWO CUP TYPE PROBES 1.5MM IN DIAMETER (GOLD COATED) TO BE TOUCHED WITH THE GOLD PADS. THE OTHER TWO PROBES WERE WITH THE 9 PINS (0.1mm IN DIAMETER) COMING OUT FROM THE PROBE CROSS SECTION SURFACE.

SAMPLE NUMBER	EXPERIMENT NUMBER	ZONE NUMBER	BULK RESISTANCE [mΩ]	CONTACT RESISTANCE [mΩ]	LASER NUMBER OF PULSES PER SITE	REMARKS
B	VII	---	4.11	---	---	FURTHER DETAILS GIVEN IN TABLE 3.2
		1		8.84; 8.18	20	
		2		7.72; 4.65	30	
C	VI		2.78			
			5.74			
		1		2.84; 2.44	20	FURTHER DETAILS GIVEN IN TABLE 3.2
		2		4.43; 3.34	20	
		3		1.74; 1.78	20	

immersed in the plating solution. Practically one can say that treatment of the ceramic material in the gold-ethanol solution did not lead to a significant change in the electrical resistance.

Typical I-V curves obtained by two probes on gold deposit lines are shown in Figure 3.18 where the results are summarized in Table 3.4. Resistance of 35.7 ohms and 45.45 ohms were found on gold deposit lines produced via pulse laser irradiation under 1000 pulses/site and 100 pulses/site respectively (see Table 3.4, Sample A, line 3,4). Resistance of about 20 ohms was found within gold deposit line number 5 where the irradiation conditions were different compared to lines 3 and 4. In line 5 probably more gold was deposited compared to the other two lines.

The results of two probes measurements of gold deposit lines on Sample B, Line 3a and 4a (See Table 3.1, Sample B, Exp. V, Line 3a, 4a) are shown in Figure 3.19 and in Table 3.5. It might be noted that the straight I-V curves indicated ohmic contact behavior between the gold line and the ceramic substrate. The resistance measured on the ceramic bulk material was found to be 12.5 ohms (Table 3.5) where the resistance of the gold deposit formed under 100 laser pulses (Table 3.5, Line 3a) was 66 ohms compared to 30 ohms of gold line deposit formed under 200 laser pulses (Table 3.5, Line 4a). The data generated at this stage of the work indicated that the gold deposit line resistance decreased with increased number laser pulses, or in other words, with the increase amount of gold deposited.

Contact resistance measurements of gold deposit pads onto the superconductor ceramic material specimens were conducted by the four

probes resistance measured as was described in Figure 2.5.B. The results obtained at ambient temperature on various gold pads are given in Table 3.6. The readings of the potential drop between the two inner probes were taken at constant current of 100 mA. Contact resistance average values of gold deposit pads on the surface of Sample B (see Table 3.6, Exp. VII, Lines 1,2) were about 8.5 mΩ on Zone No. 1 and about 6.2 mΩ on Zone No. 2.

It might be noted that gold pad No. 1 was produced under 20 pulses/site compared to 30 pulses/site in gold pad No. 2. That might explain the lower contact resistance at pad No. 2 where more gold was deposited as shown also in Figure 3.3.A. Further four probes measurements were conducted on gold deposit pads produced via pulse laser on Sample C (see Table 3.2, Sample C, Exp. VI, Zones 1,2,3). The results are summarized in Table 3.6. The average contact resistance on pad zone No. 1 was 2.64 mΩ, on pad No. 2 it was 3.88 mΩ and on pad No. 3 it was 1.76 mΩ. Although these pads on Sample C were produced under the same laser conditions, their contact resistances were between 1.76 mΩ to 2.64 mΩ and 3.88 mΩ. That can possibly be attributed to rough and porous surface of the ceramic specimen to begin with (see Figure 3.4, Figure 3.10, and Figure 3.11).

3.3.2 Contact Resistance Measurement at Low Temperature

The results of measuring gold pad contact resistance to the superconductive ceramic material as function of temperature are shown in Figure 3.20 and 3.21.

Figure 3.20 shows an increase of contact resistance with a decrease of temperature in the range of 300°K to 50°K. That behavior is

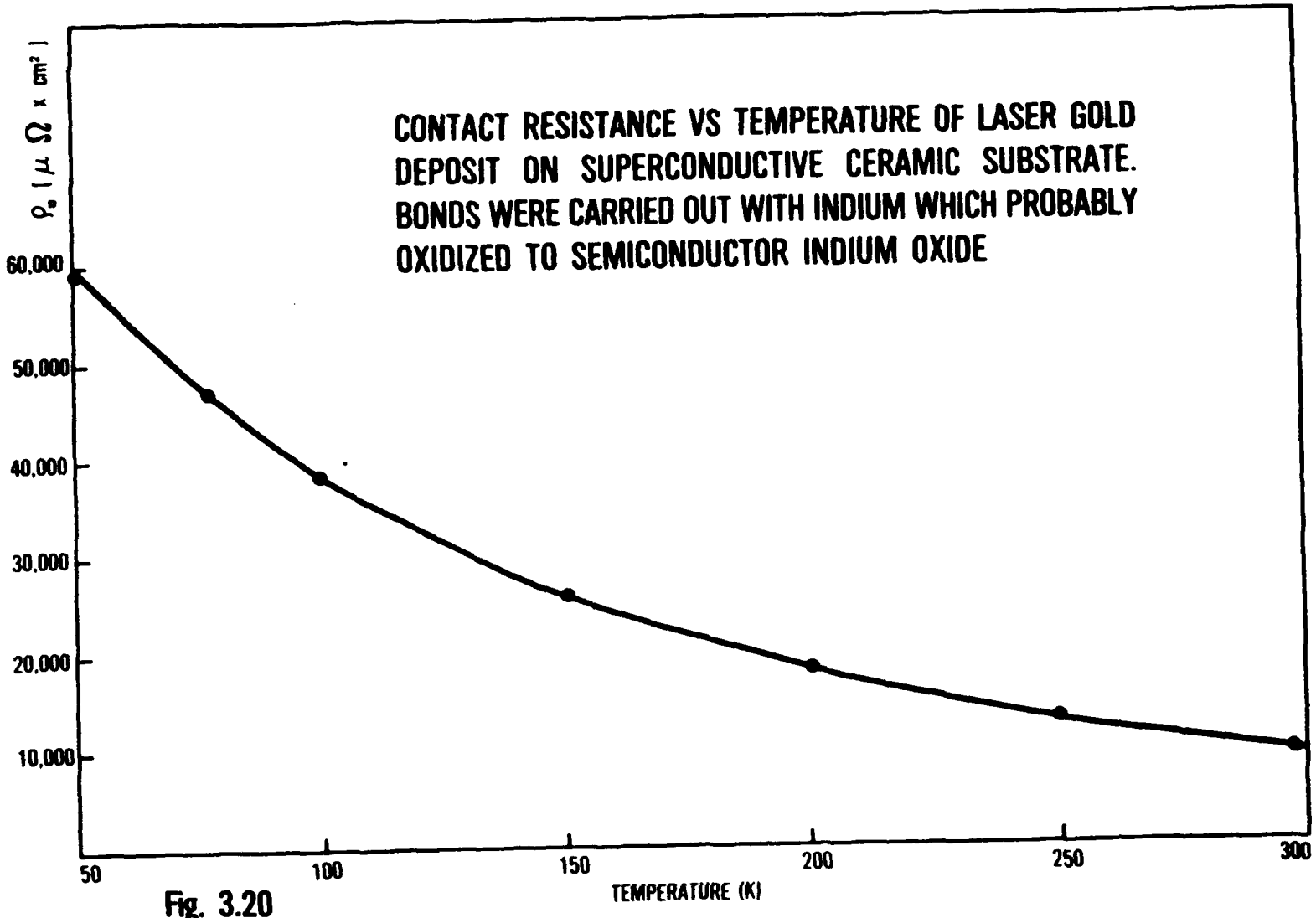

Fig. 3.20
CONTACT RESISTANCE VS TEMPERATURE OF GOLD DEPOSIT PAD [SEE TABLE 3.2, SAMPLE D, EXP VIII, SET A]. GOLD WIRE WAS CONNECTED TO THE GOLD PAD WITH INDIUM FOR MEASURING THE CONTACT RESISTANCE BETWEEN GOLD PAD AND THE SUPERCONDUCTOR Y-Ba-Cu-O CERAMIC MATERIAL.

typically for semiconductor and not for metallic contact. That type of behavior was previously reported [9] for Indium contact resistance on superconductor ceramic material. The Indium oxidized to give Indium Oxide with energy gap of about 3.4 eV [9]. The Indium oxide behave like a semiconductor. Looking into the procedure of preparing the contact of gold wire to the gold pad Indium was used to get a good connection. The presence of Indium in the system (Figure 2.7) resulted in the correlation shown in Figure 3.20.

Figure 3.21 shows the dependence of contact resistance on temperature. The measurements were carried out on gold deposits and produced via pulse laser irradiation (See Table 3.2, Sample D, Exp. VII, Set A). The connection of gold wire to the gold pad was carried out through ultrasonic pressure without any Indium. Contact resistance decreased with decrease of temperature (see Figure 3.21).

Contact resistance value at a room temperature 300°K was found around 13 $\mu\Omega \times Cm^2$ compared to 80 $\mu\Omega \times Cm^2$ reported in the literature [9,10]. The contacts obtained were ohmic. Increasing the current from 1.0 mA to up to 100 mA caused an increase in the potential drop measured to give a constant value of the resistance at given temperature. Also it might be noted that our procedure of making gold contacts did not involve annealing procedure to get low ohmic contact resistance. In comparison it was reported in the literature that sputtered gold contacts on superconductive Y-Ba-Cu-O base material should be annealed at 600°C for one hour at pressure of one atmosphere of O_2 to get low ohmic metallic contacts [9,10].

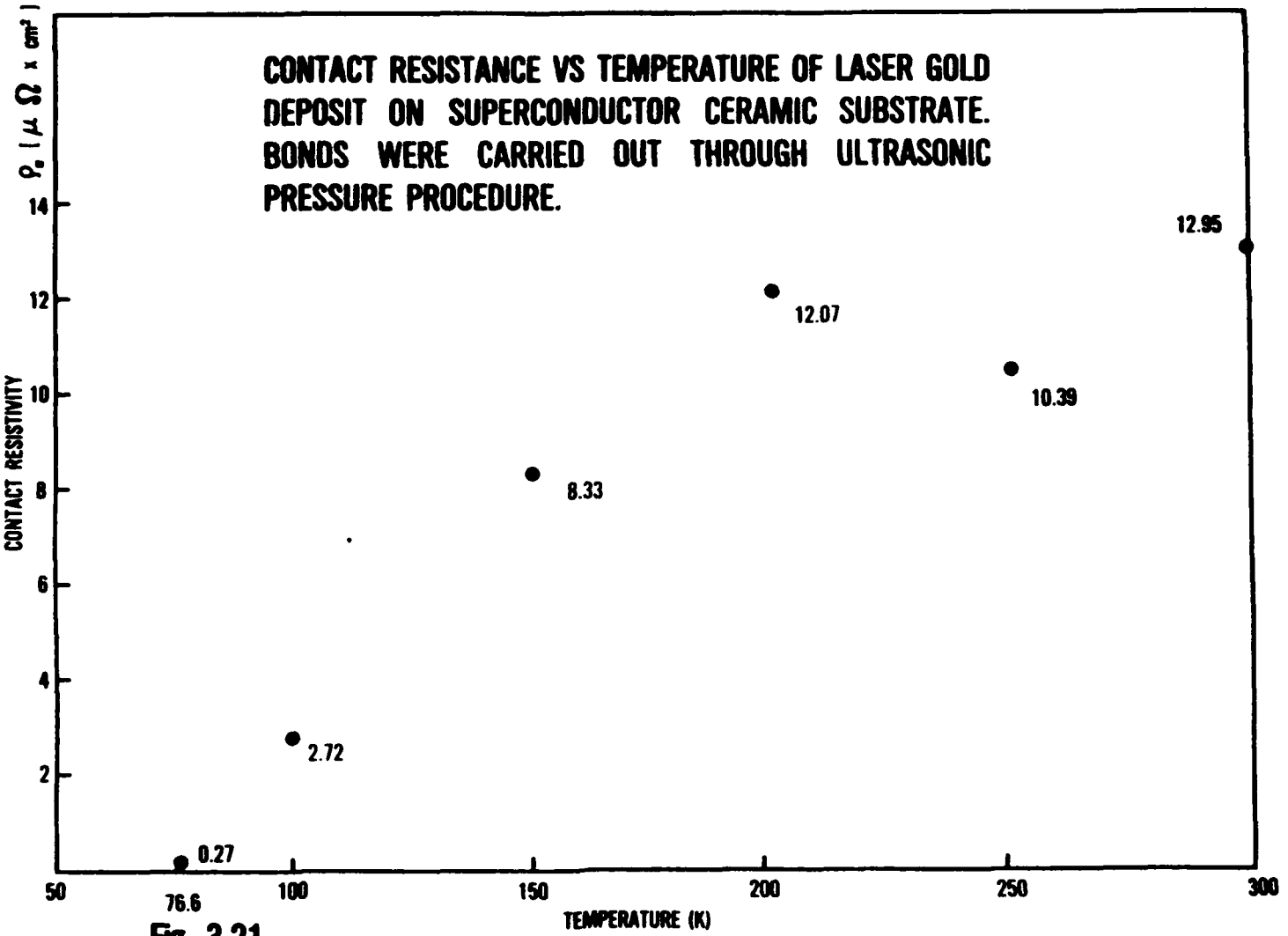

Fig. 3.21
CONTACT RESISTANCE OF GOLD DEPOSIT PAD ON SUPERCONDUCTIVE Y-Ba-Cu-O BASE CERAMIC MATERIAL AS FUNCTION OF TEMPERATURE [SEE TABLE 3.2, SAMPLE D, SET A]. THE GOLD WIRE WAS ULTRASONICALLY BONDED TO THE GOLD PAD. CONTACT RESISTANCE DECREASED WITH TEMPERATURE DECREASE INDICATING THAT THE CONTACTS ARE METALLIC IN NATURE

Further contact resistance measurement of gold pads on a super conductive ceramic substrate were conducted by two point probes and by four point probes making use of the gold pads as shown schematically in Figure 3.22. The two point probe procedure on gold pads is shown in Figure 3.22.A. There were two pads operating while the current and the voltage leads of gold wires were connected to each of the pad seperately (Figure 3.22.A). The measurement shown in Figure 3.22.A gave the combined resistance that is the contact resistance together with superconductor resistance.

In Figure 3.22.B however, the resistance measured by four point probes was basically the superconductor resistance. The results obtained of the resistance measurements both through two point probes and four point probes are shown in Figure 3.2.3. In order to get the contact resistance itself of gold pads the values obtained by four point probes were subtracted from the values obtained with two point probes. The graphic results of that subtraction is shown in Figure 3.24. Contact resistance in the order of 2 mΩ was found at room temperature similar to results obtained by four point probes measurements (see Figure 2.5.B) and reported in Table 3.6, Sample C, Exp. VI, Zones 1,2,3.

Furthermore, Figure 3.24 shows a decrease in contact resistance with decrease of temperature getting probably a jump from about 0.7 mΩ to 0.1 mΩ at transition temperature around 90°K.

These measurements of contact resistance as function of temperature are still being carried out and are investigated.

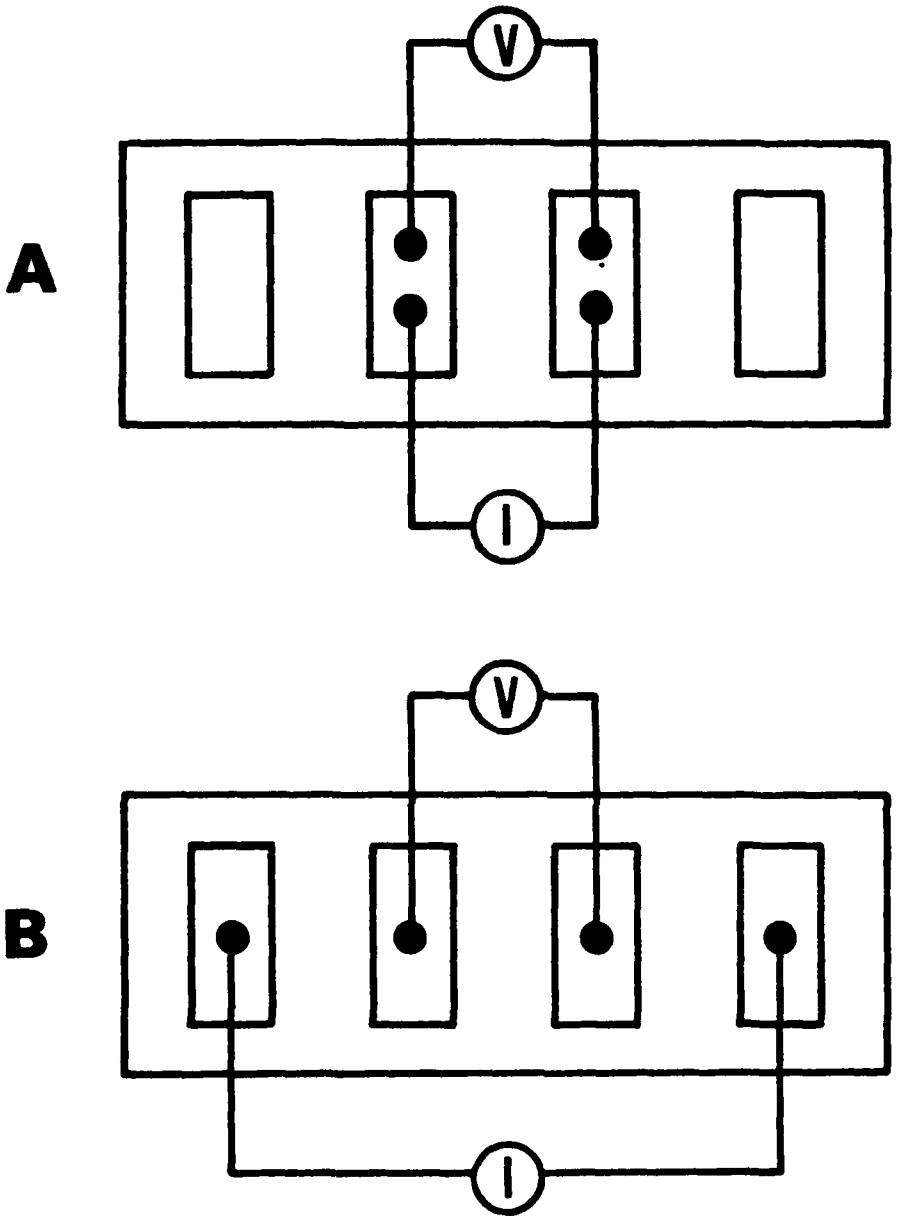

FIG. 3.22
SCHEMATIC DESCRIPTION OF (A) TWO POINT AND (B) FOUR POINT PROBES CONTACT RESISTANCE MEASUREMENT OF GOLD PADS AT VARIOUS TEMPERATURES

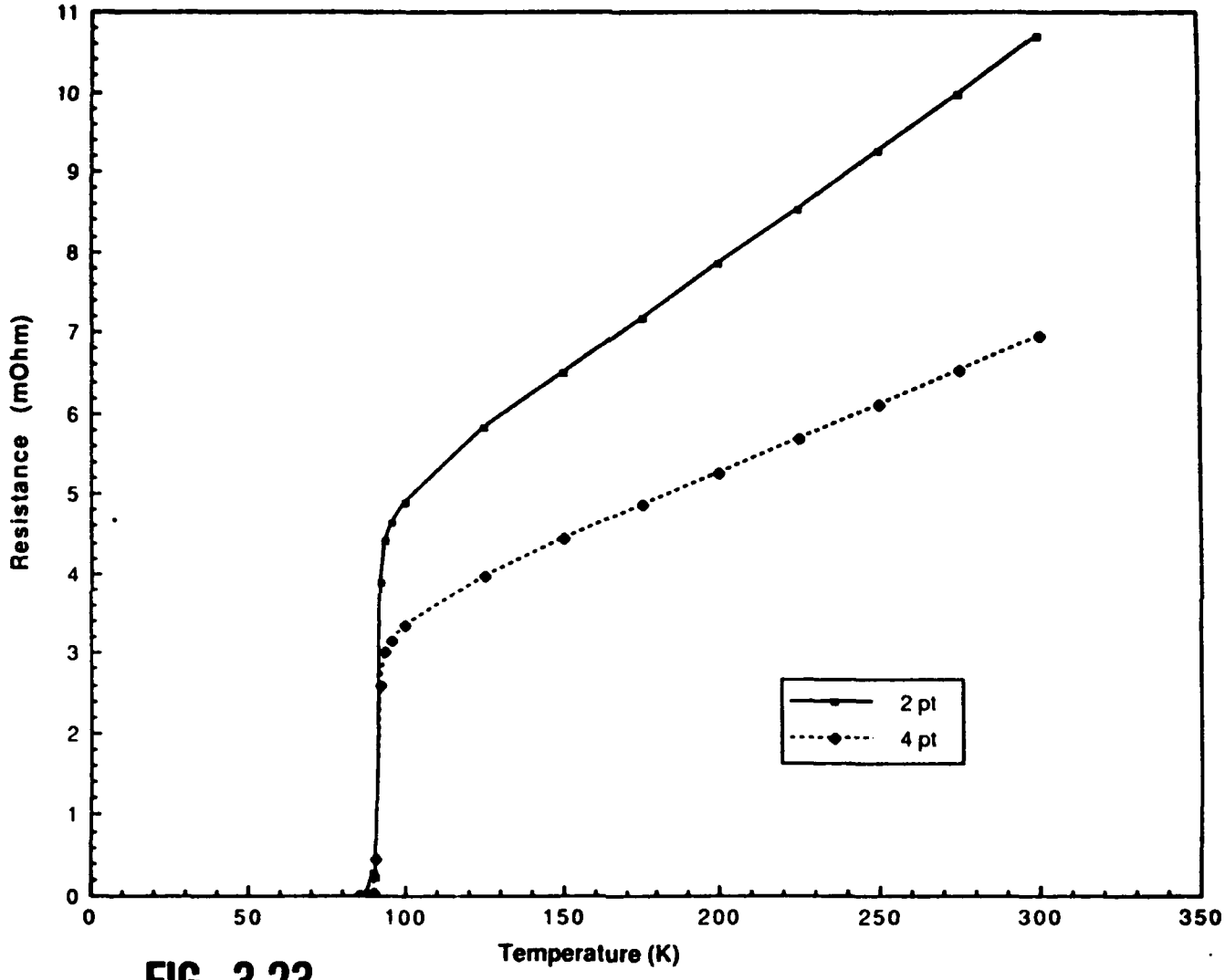

FIG. 3.23

TWO AND FOUR POINT PROBES RESISTANCE MEASUREMENTS AS FUNCTION OF TEMPERATURE

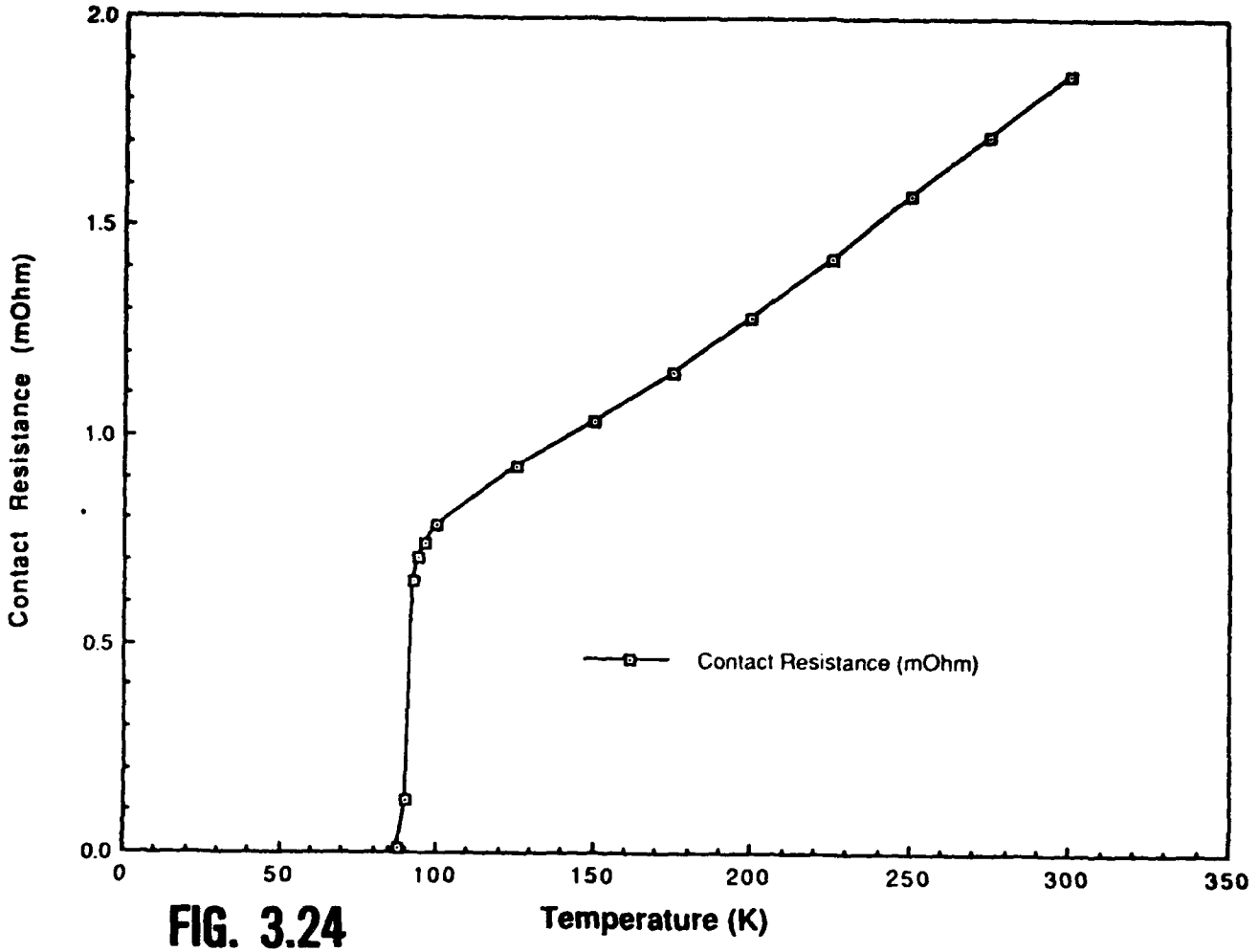

FIG. 3.24
CONTACT RESISTANCE CALCULATED FROM FIG. 3.23 [TWO POINT PROBE MEASUREMENTS MINUS FOUR POINT PROBE MEASUREMENTS] AS FUNCTION OF TEMPERATURE

4.0 CONCLUDING REMARKS

A. The feasibility of laser induced high speed, high selective metal (gold) deposit on superconductive ceramic material immersed in plating solution has been shown and proven in this study.

B. Selective, direct gold deposit formation via pulse laser irradiation was carried out from nonaqueous gold plating solution without external power or lithography procedures.

C. Gold deposit content increased with increase of laser number of pulses, overlapping percentage values, and laser energy per pulse.

D. Patterned metalizations of gold were deposited on superconductor ceramic substrate showed low resistance ohmic contact. Contact resistance decreased with decrease of temperature from R.T. to liquid N_2 temperature. At R.T. laser gold deposit contact resistance showed values around 12 $\mu\Omega \times Cm^2$ compared to 80 $\mu\Omega \times Cm^2$ found in the literature for sputtered gold [9].

5.0 REFERENCES

1. J.G. Bendorz and K.A. Muller, Z. Phys. B64,189-193, (1986).

2. S.J. Hwu, S.N. Song, J. Thiel, K.R. Poeppelmeier, J.B. Ketterson and A.J. Freeman, Physical Review B, Vol. 35, No. 13, 7119-7121, (1987).

3. J.M. Tarascon, L.H. Greene, W.R. McKinnon, and G.W. Hull, Physical Review B, Vol. 35, No. 13, 7115-7118, (1987).

4. P.M. Grant, R.B. Beyers, E.M. Engler, G. Lim, S.S.P. Parkin, M.L. Ramirez, V.Y. Lee, A. Nazzal, J.E. Varquez, and R.J. Savoy, Physical Review B, Vol. 35, No. 13, 7242-7244, (1987).

5. J.Z. Sun, D.J. Webb, M. Naito, K. Char, M.R. Hahn, J.W.P. Hsu, A.D. Kent, D.B. Mitzi, B. Oh, M.R. Beasley, T.H. Geballe, R.H. Hammond, and A.K. Kapitulnik, Physical Review Letters, Vol. 58, No. 15, 1574-1576, (1987).

6. S.B. Qadri, L.E. Toth, M. Osofsky, S. Lawrence, D.U. Gubser, and S.A. Wolf, Physical Review B., Vol. 35, No. 13, 7235-7237, (1987).

7. R.J. Cava, B. Batlogg, R.B. Van Dower, D.W. Murphy, S. Sunshine, T. Siegrist, J.P. Remeika, E.A. Rietman, S. Zahurak, and G.P. Espinosa "Bulk Superconductivity at 91K In Single Phase Oxygen Deficient Perovskite" Ba_1 Y_2 Cu_3 O_7-δ" to be published.

8. Y. Tzeng, A. Holt, and R. Ely, "High Performance Silver Ohmic Contacts to Y Ba_2 Cu_3 $O_{6+\delta}$ Superconductors," Appl. Phys. Lett. 52 (2), p. 155, January 1988.

9. J.W. Ekin, A.J. Panson and B.A. Blankenship, "Method for Making Low Resistivity Contacts to High Tc Superconductors," Appl. Phys. Lett. 52, (4), p. 331, January (1988).

10. J.W. Ekin, T.M. Larson, N.F. Bergren, A.J. Nelson, A.B. Swartzlander, and L.L. Kazmerski, "Hig Tc Superconductors/Noble-Metal Contacts With Surface Resistivities in the 10^{-10} Ω Cm^2 Range," Apl. Phys. Lett. Vol 52, No. 2., p. 1820, May (1988).

11. J.Zahavi, S. Tamir, and M. Halliwell, "Laser Induced Direct Metals Deposition on Semiconductor and Polymeric Substrates From Electroplating Solutions," J. of Plating and Surface Finishing, pp. 57-64, February (1986).

12. J. Zahavi and M. Halliwell, "Selective Gold Plating Using Laser Beams," Metal Finishing, pp. 61-64, July (1985).

13. J. Zahavi and S. Tamir, "Laser Induced Deposition on a Silicon Substrate," J. Vacuum Science Technonogy A, Vol 3., p. 2312, (1985).

14. J. Zahavi, S. Tamir and M. Halliwell "Laser Induced Metal and Alloy Plating with Simultaneous Silicide Compound Formation," Mat. Res. Soc. Symp, Proc., Vol 71, MRS pp. 387-393, May (1986).

15. J. Zahani and Pehr E. Pehrsson, "UV Laser Induced Metal Depisition on Semiconductor From Electroplating Solutions," Mat. Res. Soc. Symp. Proc., Vol 75, p.p. 173-177, May (1987).

16. R.L. Barns and R.A. Laudise, "Stability of Superconducting Y Ba_2 Cu_3 O_7 In the Presence of Water," Appl. Phys. Lett. 51 (17), p. 1373, October (1987).

17. M.F. Yan, R.L. Barns, H.M. O'Bryan,Jr., P.K. Gallapher, R.C. Sherwood, and S. Jin, "Water Interaction With the Superconducting Y_1 Ba_2 Cu_3 O_7 Phase," Appl Phys. Lett. 51 (7), p. 532, August (1987).

18. ASTM B 193-178 "Standard Test Method for Resistivity of Electrical Conductor Materials," ANSI/ASTM B193-1978, pp. 392-395.